

Quantized vortex stability and interaction in the nonlinear wave equation

Weizhu Bao^{a,b,*}, Rong Zeng^c, Yanzhi Zhang^{a,1}

^a Department of Mathematics, National University of Singapore, Singapore 117543, Singapore

^b Center for Computational Science and Engineering, National University of Singapore, Singapore 117543, Singapore

^c Department of Electrical Engineering, Tsinghua University, Beijing, 100084, China

Received 28 May 2007; received in revised form 11 March 2008; accepted 19 March 2008

Available online 25 March 2008

Communicated by B. Sandstede

Abstract

The stability and interaction of quantized vortices in the nonlinear wave equation (NLWE) are investigated both numerically and analytically. A review of the reduced dynamic law governing the motion of vortex centers in the NLWE is provided. The second order nonlinear ordinary differential equations for the reduced dynamic law are solved analytically for some special initial data. Using 2D polar coordinates, the transversely highly oscillating far field conditions can be efficiently resolved in the phase space, thus giving rise to an efficient and accurate numerical method for the NLWE with non-zero far field conditions. By applying this numerical method to the NLWE, we study the stability of quantized vortices and find numerically that the quantized vortices with winding number $m = \pm 1$ are dynamically stable, and resp. $|m| > 1$ are dynamically unstable, in the dynamics of NLWE. We then compare numerically quantized vortex interaction patterns of the NLWE with those from the reduced dynamic law qualitatively and quantitatively. Some conclusive findings are obtained, and discussions on numerical and theoretical results are made to provide further understanding of vortex stability and interactions in the NLWE. Finally, the vortex motion under an inhomogeneous potential in the NLWE is also studied.

© 2008 Elsevier B.V. All rights reserved.

Keywords: Nonlinear wave equation; Quantized vortex; Reduced dynamic law; Stability; Vortex interaction

1. Introduction

In this paper we study quantized vortex stability and interaction in the nonlinear wave equation (NLWE) [26,22]:

$$\partial_{tt}\psi(\mathbf{x}, t) = \nabla^2\psi + \frac{1}{\varepsilon^2} \left(V(\mathbf{x}) - |\psi|^2 \right) \psi, \quad \mathbf{x} \in \mathbb{R}^2, \quad (1.1)$$

$$t > 0,$$

with initial conditions

$$\psi(\mathbf{x}, 0) = \psi_0(\mathbf{x}), \quad \partial_t\psi(\mathbf{x}, 0) = \psi_1(\mathbf{x}), \quad \mathbf{x} \in \mathbb{R}^2 \quad (1.2)$$

and nonzero far field conditions

$$|\psi(\mathbf{x}, t)| \rightarrow 1, \quad (\text{e.g. } \psi \rightarrow e^{im\theta}), \quad t \geq 0,$$

$$\text{when } r = |\mathbf{x}| = \sqrt{x^2 + y^2} \rightarrow \infty. \quad (1.3)$$

Here t is time, $\mathbf{x} = (x, y)^T \in \mathbb{R}^2$ is the Cartesian coordinate vector, (r, θ) is the polar coordinate system, $\psi = \psi(\mathbf{x}, t)$ is a complex-valued order parameter (or wave function), $V(\mathbf{x})$ is a real-valued external potential satisfying $\lim_{|\mathbf{x}| \rightarrow \infty} V(\mathbf{x}) = 1$, $m \in \mathbb{Z}$ is a given integer and $\varepsilon > 0$ is a constant.

It is well known that there exist stationary *vortex solutions* with the single winding number (or index) $m \in \mathbb{Z}$ of the NLWE (1.1) with $\varepsilon = 1$ and $V(\mathbf{x}) \equiv 1$ [25,22,14], which take the form

$$\phi_m(\mathbf{x}) = f_m(r) e^{im\theta}, \quad \mathbf{x} = (r \cos \theta, r \sin \theta)^T \in \mathbb{R}^2, \quad (1.4)$$

where the modulus $f_m(r)$ is a real-valued function satisfying

$$\frac{1}{r} \frac{d}{dr} \left(r \frac{df_m(r)}{dr} \right) - \frac{m^2}{r^2} f_m(r) + \left(1 - f_m^2(r) \right) f_m(r) = 0,$$

* Corresponding author at: Department of Mathematics, National University of Singapore, Singapore 117543, Singapore. Tel.: +65 6516 2765; fax: +65 6774 6756.

E-mail addresses: bao@math.nus.edu.sg (W. Bao), zengrong@tsinghua.edu.cn (R. Zeng), yizhang@scs.fsu.edu (Y. Zhang).
URL: <http://www.math.nus.edu.sg/~bao/> (W. Bao).

¹ Current address: School of Computational Science, Florida State University, Tallahassee, FL 32306-4120, USA.

$$0 < r < \infty, \quad (1.5)$$

$$f_m(0) = 0, \quad f_m(r) = 1, \quad \text{when } r \rightarrow \infty. \quad (1.6)$$

Numerical solutions of the modulus for different winding numbers m were reported in the literature [25,34,35] by solving the boundary value problem (1.5)–(1.6) numerically. In addition, the core size r_m^0 of a vortex state with winding number m is defined by the condition $f_m(r_m^0) = 0.755$, and then when $m = \pm 1$, the core size $r_1^0 \approx 1.75$ [34,35]. In fact, the quantized vortex state (1.4) satisfying the nonzero far field condition (1.3) is usually called as “bright-tail” vortex which was also widely studied in superfluid Helium [25,12,22,23,5,34,35], superconductors [25,22,15,34,35], etc. On the other hand, the quantized vortex state (1.4) decaying to zero at far field, i.e.

$$|\psi(\mathbf{x}, t)| \rightarrow 0, \quad t \geq 0, \quad \text{when } r \rightarrow \infty, \quad (1.7)$$

is usually called the “dark-tail” vortex, and has been widely studied in Bose–Einstein condensation in trapped atomic gases at ultra-low temperatures [3,24,21,1,10,9,8,17,18,36], nonlinear optics [31,32], etc.

Quantized vortices have a long history that begins with the study of liquid Helium and superconductors. Their appearance is viewed as a typical signature of superfluidity which describe a phase of matter characterized by the complete absence of viscosity. The examples of superfluidity can be found in liquid Helium, Bose–Einstein condensation, superconductivity and nonlinear optics, etc. In 1955, Feynman [13] made the prediction that a superfluid rotation may be subject to an array of quantized singularities, namely, the quantized vortices. The seminal work of Abrikosov [2] in 1957 already made predictions of the vortex lattice in superconductors a decade before the experimental confirmation. Research on the quantized vortex phenomena has since flourished and it was recently highlighted by the Nobel Prizes in Physics awarded to Cornell, Weimann and Ketterle in 2001 and to Ginzburg, Abrikosov and Leggett in 2003, who have made decisive contributions to Bose–Einstein condensation, superfluidity and superconductivity and to the understanding of the quantized vortex states. In recent years, there have been many works on the numerical simulations and mathematical analysis for quantized vortex states in superfluidity and superconductivity. It is truly remarkable that many of the phenomenological properties of quantized vortices have been well captured by relatively simple mathematical models, for example, the Gross–Pitaevskii equations [29,7] and the Ginzburg–Landau equations [11,4]. The structures of quantized vortex states have been studied through various approaches ranging from asymptotic analysis, numerical simulations and rigorous mathematical analysis. Despite the great progress made in the last decade on quantized vortex states in superfluidity and superconductivity, it should be pointed out that the efficient computation and rigorous mathematical study of a large part of the subject on vortex dynamics and interaction remains nearly non-existent. Indeed, what has become available in the literature are primarily studies of the various dynamical laws of well separated vortices deduced

from the Ginzburg–Landau–Schrodinger equations [25,12,23,34,35,16,27,28,20,33] or the Gross–Pitaevskii equation with weak interaction [19,30]. On the other hand, numerical simulations have become useful tools that could help in providing a more clear picture on the exotic vortex dynamics and interaction driven by various forces, even though there are also challenging computational issues to be tackled. Thus understanding numerically and mathematically the dynamics and interaction of quantized vortices in superfluidity and superconductivity bears tremendous importance both scientifically and technologically.

The aim of this paper is first to study numerically the stability of quantized vortex solutions (1.4) of NLWE and then to investigate analytically and numerically the interaction patterns of several quantized vortices with winding number $m = \pm 1$ in NLWE, i.e., we study (1.1) with initial conditions in (1.2) containing several vortices, which take the form

$$\psi_0(\mathbf{x}) = \prod_{j=1}^N \phi_{m_j}(\mathbf{x} - \mathbf{x}_j^0) = \prod_{j=1}^N \phi_{m_j}(x - x_j^0, y - y_j^0), \quad \mathbf{x} \in \mathbb{R}^2. \quad (1.8)$$

Here N is the total number of vortices, ϕ_{m_j} is the vortex state in (1.4) with winding number $m_j = \pm 1$ (see [25,34] for their numerical solutions), and $\mathbf{x}_j^0 = (x_j^0, y_j^0)^T$ is the initial location of the j -th ($1 \leq j \leq N$) vortex center. That is, we consider the interaction of N vortices by shifting their initial centers from the origin $(0, 0)^T$ to \mathbf{x}_j^0 ($1 \leq j \leq N$). Taking $m = \sum_{j=1}^N m_j$ in (1.3), we refer to vortices with the same winding numbers as *like vortices* while those with different winding numbers as *opposite vortices*.

In fact, vortex dynamics for NLWE is a typical model of the “particle and field” theories of classical physics. The formal derivation of the reduced dynamic law was done by Neu [26] for NLWE (1.1) with $\varepsilon = 1$ and $V(\mathbf{x}) \equiv 1$. In this case, for N well-separated vortices of winding numbers $m_j = \pm 1$ ($1 \leq j \leq N$), he obtained asymptotically the following second order nonlinear ordinary differential equations (ODEs) for the reduced dynamic law governing the induced motion of the N vortex centers $\mathbf{x}_j(t)$ ($1 \leq j \leq N$) in the leading order, i.e. the adiabatic approximation [26], as

$$\kappa \mathbf{x}_j''(t) = 2m_j \sum_{l=1, l \neq j}^N m_l \frac{\mathbf{x}_j(t) - \mathbf{x}_l(t)}{|\mathbf{x}_j(t) - \mathbf{x}_l(t)|^2}, \quad t \geq 0, \quad (1.9)$$

$$\mathbf{x}_j(0) = \mathbf{x}_j^0, \quad \mathbf{x}_j'(0) = \mathbf{x}_j^1, \quad 1 \leq j \leq N, \quad (1.10)$$

where κ is a constant determined from the initial setup (1.8). He also made an interesting connection between vortex dynamics and the Dirac theory of electrons [26]. Later, Lin [22] gave a rigorous mathematical proof of the reduced dynamic law with a correction term denoting the residuals of a holomorphic function defined away from the vortices. Here we will solve the second order nonlinear ODEs (1.9) for some special initial data in (1.10). These solutions will provide qualitatively the interaction patterns of quantized vortices in NLWE. By proposing an efficient and accurate numerical method for

NLWE, we can also study numerically vortex interaction patterns by directly simulating NLWE and compare them with those from the reduced dynamic law qualitatively and quantitatively.

The paper is organized as follows. In Section 2, based on the second order nonlinear ODEs of the reduced dynamic law, we prove the conservation of the mass center and mean velocity of the N vortex centers under certain conditions, and solve analytically the reduced dynamic law with a few types of initial data. In Section 3, an efficient and accurate numerical method is proposed for simulating NLWE and the stability of quantized vortices is reported. In Section 4, the interactions of quantized vortices in NLWE with zero initial velocity are obtained by directly simulating (1.1) and compared with those from the reduced dynamic law. In Section 5, the interactions of quantized vortices with nonzero initial velocity and the dynamics of vortex state under an inhomogeneous external potential are reported. Finally, some conclusions are drawn in Section 6.

2. The reduced dynamic law and its solutions

In this section, we first prove the conservation of the mass center and mean velocity of the N vortex centers in the reduced dynamic law (1.9) under certain conditions. These conservation properties can be used to solve the dynamic law in special cases and to compare with the direct numerical simulation of NLWE. We then solve the second order nonlinear ODEs (1.9)–(1.10) analytically for several types of initial data, and such analytical solutions can again be compared with the numerical solutions of NLWE.

2.1. Conservation laws

Define respectively the mass center $\bar{\mathbf{x}}(t)$ and the mean velocity $\bar{\mathbf{v}}(t)$ of the N vortex centers as

$$\bar{\mathbf{x}}(t) := \frac{1}{N} \sum_{j=1}^N \mathbf{x}_j(t), \quad \text{and} \tag{2.1}$$

$$\bar{\mathbf{v}}(t) := \bar{\mathbf{x}}'(t) = \frac{1}{N} \sum_{j=1}^N \mathbf{x}'_j(t).$$

Then we have

Lemma 2.1. *The mean velocity of the N vortex centers in the reduced dynamic law (1.9) for NLWE is conserved, i.e.*

$$\bar{\mathbf{v}}(t) := \frac{1}{N} \sum_{j=1}^N \mathbf{x}'_j(t) \equiv \bar{\mathbf{v}}(0) := \frac{1}{N} \sum_{j=1}^N \mathbf{x}'_j(0) = \frac{1}{N} \sum_{j=1}^N \mathbf{x}_j^1, \tag{2.2}$$

$t \geq 0.$

In addition, the dynamics of the mass center of the N vortices in the reduced dynamic law (1.9) for NLWE satisfies

$$\begin{aligned} \bar{\mathbf{x}}(t) &:= \frac{1}{N} \sum_{j=1}^N \mathbf{x}_j(t) = \bar{\mathbf{x}}(0) + t \bar{\mathbf{v}}(0) \\ &= \frac{1}{N} \sum_{j=1}^N \mathbf{x}_j^0 + t \left(\frac{1}{N} \sum_{j=1}^N \mathbf{x}_j^1 \right), \quad t \geq 0, \end{aligned} \tag{2.3}$$

which immediately implies that the mass center is conserved if $\bar{\mathbf{v}}(0) = 0$, and respectively, it moves to infinity starting from the initial mass center $\bar{\mathbf{x}}(0)$ along the direction of the initial mean velocity $\bar{\mathbf{v}}(0)$ if $\bar{\mathbf{v}}(0) \neq 0$.

Proof. Summing (1.9) for $1 \leq j \leq N$ and noticing (2.1), we get for $t \geq 0$,

$$\begin{aligned} \bar{\mathbf{v}}'(t) &= \bar{\mathbf{x}}''(t) = \frac{1}{N} \sum_{j=1}^N \mathbf{x}''_j(t) \\ &= \frac{1}{N} \sum_{j=1}^N \frac{2m_j}{\kappa} \sum_{l=1, l \neq j}^N m_l \frac{\mathbf{x}_j(t) - \mathbf{x}_l(t)}{|\mathbf{x}_j(t) - \mathbf{x}_l(t)|^2} \\ &= \frac{2}{\kappa N} \sum_{j=1}^{N-1} \sum_{j < l \leq N} m_j m_l \\ &\quad \times \left[\frac{\mathbf{x}_j(t) - \mathbf{x}_l(t)}{|\mathbf{x}_j(t) - \mathbf{x}_l(t)|^2} + \frac{\mathbf{x}_l(t) - \mathbf{x}_j(t)}{|\mathbf{x}_l(t) - \mathbf{x}_j(t)|^2} \right] \\ &= 0, \quad t \geq 0. \end{aligned} \tag{2.4}$$

Thus the conservation of the mean velocity in (2.2) is a combination of the above and (1.10). Plugging (2.2) into (2.1), we obtain

$$\bar{\mathbf{x}}'(t) = \bar{\mathbf{v}}(t) \equiv \bar{\mathbf{v}}(0), \quad t \geq 0. \tag{2.5}$$

Integrating the above and noticing (1.10), we get (2.3) immediately. \square

2.2. Analytical solutions of the reduced dynamic law

Noticing (2.2) and (2.3), we can solve the second order nonlinear ODEs (1.9) analytically for some special initial data in (1.10). Without loss of generality, in these cases, we assume that the initial mass center is at the origin, i.e. $\bar{\mathbf{x}}(0) = (0, 0)^T$, and denote θ_0 as a given constant and $m_0 = +1$ or -1 .

Lemma 2.2. *If the initial data in (1.10) satisfies for $1 \leq j \leq N$*

$$\begin{aligned} \mathbf{x}_j^0 &= a \left(\cos \left(\frac{2j\pi}{N} + \theta_0 \right), \sin \left(\frac{2j\pi}{N} + \theta_0 \right) \right)^T, \\ \mathbf{x}_j^1 &= (0, 0)^T, \quad m_j = m_0, \end{aligned} \tag{2.6}$$

*i.e. the N ($N \geq 2$) like vortices are uniformly located on a circle and there is no initial velocity (denoted as **Pattern I**), then the solutions of (1.9)–(1.10) can be given, for $1 \leq j \leq N$ with $N \geq 2$, by*

$$\begin{aligned} \mathbf{x}_j(t) &= c_N(t) \left(\cos \left(\frac{2j\pi}{N} + \theta_0 \right), \sin \left(\frac{2j\pi}{N} + \theta_0 \right) \right)^T \\ &= \frac{c_N(t)}{a} \mathbf{x}_j^0, \quad t \geq 0, \end{aligned} \tag{2.7}$$

where $c_N(t)$ satisfies the following second order ODE

$$\begin{aligned} c_N''(t)c_N(t) &= \frac{N-1}{\kappa}, \quad t \geq 0, \quad c_N(0) = a, \\ c_N'(0) &= 0; \end{aligned} \tag{2.8}$$

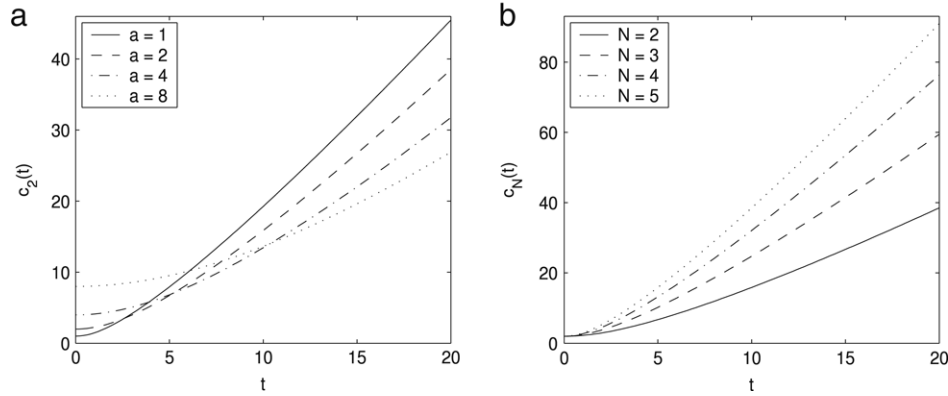


Fig. 1. Numerical solutions of the ODE (2.8) with $\kappa = 1$ for: (a) different a with $N = 2$, and (b) different N with $a = 2$.

or the following first order ODE

$$c'_N(t) = \sqrt{2(N-1)/\kappa} \sqrt{\ln[c_N(t)/a]}, \quad t \geq 0, \tag{2.9}$$

$$c_N(0) = a.$$

Proof. For simplicity, we first consider the case of $N = 2$. By conservation of the mass center, we have

$$\mathbf{x}_1(t) = -\mathbf{x}_2(t), \quad t \geq 0. \tag{2.10}$$

Plugging (2.10) into (1.9) with $N = 2$, we get for $1 \leq j \leq 2$

$$\kappa \mathbf{x}''_j(t) = \frac{\mathbf{x}_j(t)}{|\mathbf{x}_j(t)|^2}, \quad t \geq 0, \text{ with } \mathbf{x}_j(0) = \mathbf{x}^0_j, \tag{2.11}$$

$$\mathbf{x}'_j(0) = \mathbf{x}^1_j = (0, 0)^T.$$

Based on the structure of the ODEs (2.11), we take the ansatz for the solution as

$$\mathbf{x}_j(t) = \frac{c_2(t)}{a} \mathbf{x}^0_j, \quad t \geq 0, 1 \leq j \leq 2, \tag{2.12}$$

where $c_2(t)$ is a function of time t satisfying $c_2(0) = a$ and $c'_2(0) = 0$. Substituting (2.12) into (2.11) and applying the dot-product at both sides by \mathbf{x}^0_j , noticing (2.6) with $N = 2$, we get (2.8) for $N = 2$ immediately. For the cases of $N > 2$, we can generalize the solution (2.12) as

$$\mathbf{x}_j(t) = \frac{c_N(t)}{a} \mathbf{x}^0_j, \quad t \geq 0, 1 \leq j \leq N, \tag{2.13}$$

where $c_N(t)$ is a function of time t satisfying $c_N(0) = a$ and $c'_N(0) = 0$. Substituting (2.13) into (1.9) and applying dot-product at both sides by \mathbf{x}^0_j , noticing (2.6), we get

$$c''_N(t) = \frac{2}{\kappa c_N(t)} \sum_{l=1, l \neq j}^N m_j m_l \frac{(\mathbf{x}^0_j - \mathbf{x}^0_l) \cdot \mathbf{x}^0_j}{|\mathbf{x}^0_j - \mathbf{x}^0_l|^2}$$

$$= \frac{2}{\kappa c_N(t)} \sum_{l=1, l \neq j}^N \frac{a^2 - \mathbf{x}^0_l \cdot \mathbf{x}^0_j}{2a^2 - 2\mathbf{x}^0_l \cdot \mathbf{x}^0_j}$$

$$= \frac{N-1}{\kappa c_N(t)}, \quad t \geq 0. \tag{2.14}$$

Thus, the solution (2.7) is a combination of (2.13), (2.14) and (2.6). \square

Fig. 1 shows numerical results of the second order ODE (2.8) with $\kappa = 1$ for different N and a by using the standard second order finite difference discretization for (2.8). From the results in Lemma 2.2 and Fig. 1, we can see that, when the N vortices are uniformly located on a circle with zero velocity initially, by the reduced dynamic law, each vortex moves outside along the line passing through its initial location and the origin, and these N vortices are located on a circle at any time t with its radius increasing with time as $c_N(t)$ in (2.8). In addition, from our numerical results, for any $\delta > 0$, we observe that (cf. Fig. 1)

$$C_1 \frac{N-1}{a^{2\kappa}} t^{1-\delta} \leq c_N(t) \leq C_2 \frac{N-1}{a^{2\kappa}} t^{1+\delta}, \quad t \gg 1,$$

where C_1 and C_2 are two generic positive constants independent of N and a .

Lemma 2.3. *If the initial data in (1.10) satisfies*

$$\mathbf{x}^0_N = (0, 0)^T, \quad \mathbf{x}^1_N = (0, 0)^T, \quad m_N = m_0, \tag{2.15}$$

and for $1 \leq j \leq N - 1$,

$$\mathbf{x}^0_j = a \left(\cos \left(\frac{2j\pi}{N-1} + \theta_0 \right), \sin \left(\frac{2j\pi}{N-1} + \theta_0 \right) \right)^T,$$

$$\mathbf{x}^1_j = (0, 0)^T, \quad m_j = m_0, \tag{2.16}$$

i.e. the N ($N \geq 3$) like vortices are uniformly located on a circle and its center and there is no initial velocity (denoted as **Pattern II**), then the solutions of (1.9) and (1.10) are:

$$\mathbf{x}_N(t) \equiv (0, 0)^T, \quad t \geq 0, \tag{2.17}$$

and for $1 \leq j \leq N - 1$ with $N \geq 3$,

$$\mathbf{x}_j(t) = d_N(t) \left(\cos \left(\frac{2j\pi}{N-1} + \theta_0 \right), \sin \left(\frac{2j\pi}{N-1} + \theta_0 \right) \right)^T$$

$$= \frac{d_N(t)}{a} \mathbf{x}^0_j, \quad t \geq 0, \tag{2.18}$$

where $d_N(t)$ satisfies the following second order ODE

$$d''_N(t) d_N(t) = \frac{N}{\kappa}, \quad t \geq 0, \quad d_N(0) = a, \quad d'_N(0) = 0; \tag{2.19}$$

or the following first order ODE

$$d'_N(t) = \sqrt{2N/\kappa} \sqrt{\ln[d_N(t)/a]}, \quad t \geq 0, \quad d_N(0) = a. \tag{2.20}$$

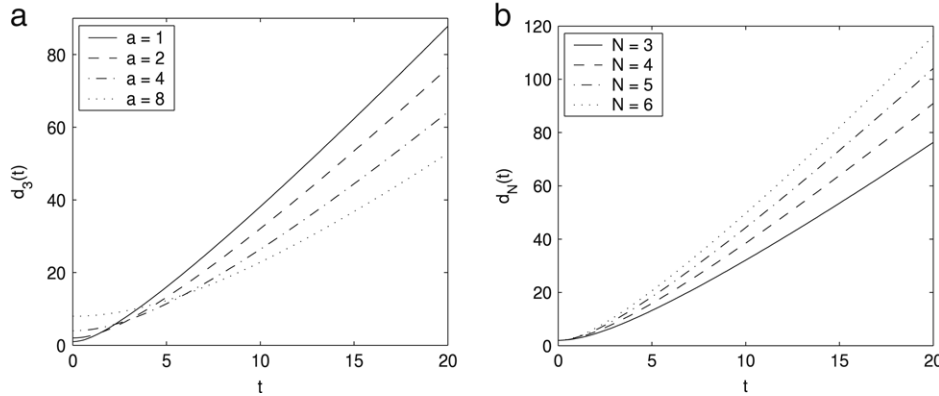


Fig. 2. Numerical solutions of the ODE (2.19) with $\kappa = 1$ for: (a) different a with $N = 3$, and (b) different N with $a = 2$.

Proof. Due to symmetry of the ODEs (1.9), the initial data (2.15)–(2.16), and the conservation of mass center (2.3) and mean velocity (2.2), we can get the solution (2.17) immediately. Similar as in the proof of Lemma 2.2, we assume

$$\mathbf{x}_j(t) = \frac{d_N(t)}{a} \mathbf{x}_j^0, \quad t \geq 0, 1 \leq j \leq N - 1, \quad (2.21)$$

where $d_N(t)$ is a function of time t satisfying $d_N(0) = a$ and $d'_N(0) = 0$. Substituting (2.21) into (1.9) and applying dot-product at both sides by \mathbf{x}_j^0 , noticing (2.16), we get

$$\begin{aligned} d''_N(t) &= \frac{2}{\kappa d_N(t)} \left[m_j m_N \frac{(\mathbf{x}_j^0 - \mathbf{x}_N^0) \cdot \mathbf{x}_j^0}{|\mathbf{x}_j^0 - \mathbf{x}_N^0|^2} \right. \\ &\quad \left. + \sum_{l=1, l \neq j}^{N-1} m_j m_l \frac{(\mathbf{x}_j^0 - \mathbf{x}_l^0) \cdot \mathbf{x}_j^0}{|\mathbf{x}_j^0 - \mathbf{x}_l^0|^2} \right] \\ &= \frac{2}{\kappa d_N(t)} \left[m_0^2 + \sum_{l=1, l \neq j}^{N-1} \frac{a^2 - \mathbf{x}_l^0 \cdot \mathbf{x}_j^0}{2a^2 - 2\mathbf{x}_l^0 \cdot \mathbf{x}_j^0} \right] \\ &= \frac{2}{\kappa d_N(t)} \left[1 + \frac{N-2}{2} \right] \\ &= \frac{N}{\kappa d_N(t)}, \quad t \geq 0. \end{aligned} \quad (2.22)$$

Thus, the solution (2.18) is a combination of (2.21), (2.22) and (2.16). \square

Fig. 2 shows numerical results of the second order ODE (2.19) with $\kappa = 1$ for different N and a . From the results in Lemma 2.3 and Fig. 2, we can see that, for the dynamics of (1.9)–(1.10) in Pattern II, by the reduced dynamic law, the vortex initially at the center of the circle does not move for any time $t \geq 0$, each of the other $N - 1$ vortices moves outside along the line passing through its initial location and the origin, and these $N - 1$ vortices are located on a circle at any time t with its radius increasing with time as $d_N(t)$ in (2.19). Again, from our numerical results, for any $\delta > 0$, we observe that (cf. Fig. 2)

$$C_1 \frac{N}{a^{2\kappa}} t^{1-\delta} \leq d_N(t) \leq C_2 \frac{N}{a^{2\kappa}} t^{1+\delta}, \quad t \gg 1.$$

Lemma 2.4. If the initial data in (1.10) satisfies the same as (2.15) and (2.16) except $m_N = -m_0$ for the center vortex, i.e. the N ($N \geq 3$) opposite vortices are uniformly located on a circle and its center and there is no initial velocity (denoted as **Pattern III**), then the solutions of (1.9)–(1.10) are:

$$\mathbf{x}_N(t) \equiv (0, 0)^T, \quad t \geq 0, \quad (2.23)$$

and for $1 \leq j \leq N - 1$ with $N \geq 3$,

$$\begin{aligned} \mathbf{x}_j(t) &= g_N(t) \left(\cos \left(\frac{2j\pi}{N-1} + \theta_0 \right), \sin \left(\frac{2j\pi}{N-1} + \theta_0 \right) \right)^T \\ &= \frac{g_N(t)}{a} \mathbf{x}_j^0, \quad t \geq 0, \end{aligned} \quad (2.24)$$

where $g_N(t)$ satisfies the following second order ODE

$$\begin{aligned} g''_N(t) g_N(t) &= \frac{N-4}{\kappa}, \quad t \geq 0, \quad g_N(0) = a, \\ g'_N(0) &= 0; \end{aligned} \quad (2.25)$$

or the following first order ODE

$$g'_N(t) = \alpha_N \sqrt{\ln [d_N(t)/a]}, \quad t \geq 0, \quad c_N(0) = a, \quad (2.26)$$

with

$$\alpha_N = \begin{cases} -\sqrt{2/\kappa}, & N = 3, \\ 0, & N = 4, \\ \sqrt{2(N-4)/\kappa}, & N \geq 5. \end{cases}$$

The proof follows the analogous results in Lemma 2.3. Fig. 3 shows numerical results of the second order ODE (2.25) with $\kappa = 1$ for different N and a . From the results in Lemma 2.4 and Fig. 3, we can see that, for the dynamics of (1.9) and (1.10) in Pattern III, by the reduced dynamic law: (i) the vortex initially at the origin does not move during the interaction, each of the other $N - 1$ vortices moves along the line passing through its initial location and the origin, and these $N - 1$ vortices are located on a circle at any time t ; (ii) when $N = 3$, the two vortices with the same index move towards each other and collide with the vortex having opposite index at the origin at finite time $t = t_c$; (iii) when $N = 4$, all the four vortices do not move and stay at their initial locations for any $t \geq 0$, and (iv) when $N \geq 5$, the $N - 1$ vortices with the same index move outside and they never collide with the vortex with the opposite

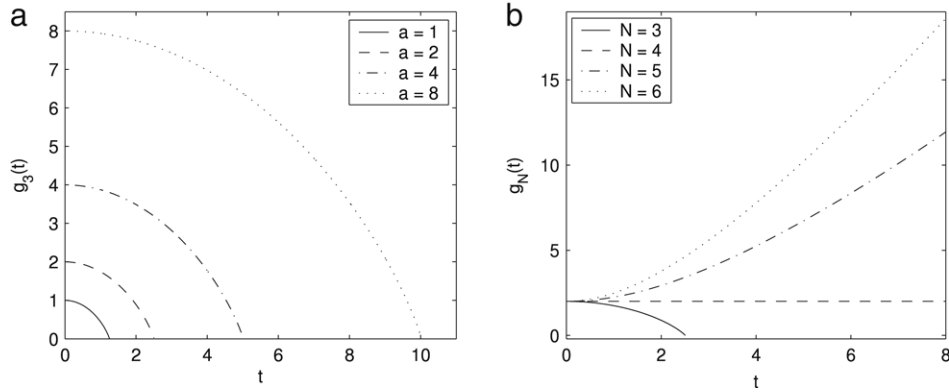


Fig. 3. Numerical solutions of the ODE (2.25) with $\kappa = 1$ for: (a) different a with $N = 3$, and (b) different N with $a = 2$.

index no matter how small the initial radius of the circle is. Again, from our numerical results, we observe that, for $N = 3$, the collision time satisfies (cf. Fig. 3(a))

$$t_c = O(a), \quad a \gg 1,$$

and for $N \geq 5$, for any $\delta > 0$, we have (cf. Fig. 3(b))

$$C_1 \frac{N-4}{a^2 \kappa} t^{1-\delta} \leq g_N(t) \leq C_2 \frac{N-4}{a^2 \kappa} t^{1+\delta}, \quad t \gg 1.$$

Lemma 2.5. *If the initial data in (1.10) satisfies for $j = 1, 2$*

$$\begin{aligned} \mathbf{x}_j^0 &= a (\cos(j\pi + \theta_0), \sin(j\pi + \theta_0))^T, \quad \mathbf{x}_j^1 = (0, 0)^T, \\ m_1 &= -m_2 = m_0, \end{aligned} \quad (2.27)$$

*i.e. two opposite vortices (denoted as **Pattern IV**), then the solutions of (1.9)–(1.10) can be given, for $j = 1, 2$, by*

$$\begin{aligned} \mathbf{x}_j(t) &= h_N(t) (\cos(j\pi + \theta_0), \sin(j\pi + \theta_0))^T \\ &= \frac{h_N(t)}{a} \mathbf{x}_j^0, \quad 0 \leq t \leq t_c, \end{aligned} \quad (2.28)$$

where $h_N(t)$ satisfies the following second order ODE

$$\begin{aligned} h_N''(t)h_N(t) &= -\frac{1}{\kappa}, \quad t \geq 0, \quad h_N(0) = a, \\ h_N'(0) &= 0; \end{aligned} \quad (2.29)$$

or the following first order ODE

$$h_N'(t) = -\sqrt{2/\kappa} \sqrt{\ln[h_N(t)/a]}, \quad t \geq 0, \quad h_N(0) = a. \quad (2.30)$$

The proof is similar to that of Lemma 2.2 with $N = 2$. Fig. 4 shows numerical results of the second order ODE (2.29) with $\kappa = 1$ for different a . From the results in Lemma 2.5 and Fig. 4, we can see that, for the dynamics of (1.9)–(1.10) in Pattern IV, when $0 \leq t < t_c$, the two vortices move towards each other along a line passing through their initial locations and collide at the origin at time $t = t_c$ according to the reduced dynamic law. Again, from our numerical results, we observe that the collision time satisfies (cf. Fig. 4)

$$t_c = O(a), \quad a \gg 1. \quad (2.31)$$

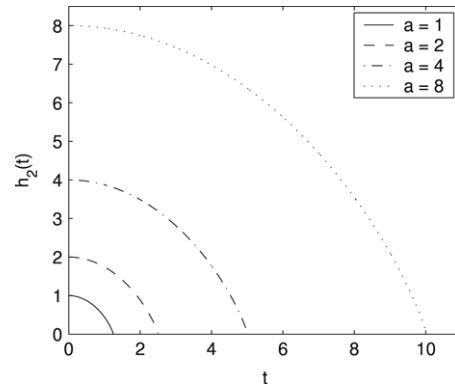


Fig. 4. Numerical solutions of the ODE (2.29) with $\kappa = 1$ for different a .

3. Numerical method and stability of vortex solutions

In this section, we first propose an efficient and accurate numerical method to discretize NLWE (1.1) with (1.2)–(1.3) and then apply it to study numerically the stability of the quantized vortex state solution (1.4) of NLWE (1.1).

3.1. An efficient and accurate numerical method

In the practical implementation, we truncate the problem (1.1)–(1.3) to one defined in a bounded computational domain with an inhomogeneous Dirichlet boundary condition:

$$\begin{aligned} \partial_{tt} \psi(\mathbf{x}, t) &= \nabla^2 \psi + \frac{1}{\varepsilon^2} (V(\mathbf{x}) - |\psi|^2) \psi, \quad \mathbf{x} \in \Omega_R, \\ &t > 0, \end{aligned} \quad (3.1)$$

$$\psi(\mathbf{x}, t) = e^{im\theta}, \quad \mathbf{x} \in \Gamma = \partial\Omega_R, \quad t \geq 0, \quad (3.2)$$

$$\psi(\mathbf{x}, 0) = \psi_0(\mathbf{x}), \quad \partial_t \psi(\mathbf{x}, 0) = \psi_1(\mathbf{x}), \quad \mathbf{x} = \bar{\Omega}_R, \quad (3.3)$$

where we choose $\Omega_R = \{(x, y), r = \sqrt{x^2 + y^2} < R\}$ with R sufficiently large. In our simulations, a sufficiently large R is chosen to assure that the effect of domain truncation remains insignificant. The use of more sophisticated radiation boundary conditions is an interesting topic that remains to be examined in the future.

To match the highly oscillatory boundary condition (3.2) in the transverse direction when m is large, we use the polar coordinate (r, θ) , and discretize (3.1)–(3.3) in θ -direction by

the Fourier pseudospectral method, in r -direction by finite difference or finite element method and in time by the second order central finite difference method. Choose a time step $\Delta t > 0$ and a mesh size in θ -direction $\Delta\theta = 2\pi/K > 0$ with K an even positive integer. Denote the grid points as $\theta_k = k\Delta\theta$ for $0 \leq k \leq K$, and time sequence as $t_n = n\Delta t$ for $n = 0, 1, \dots$; let $0 < r_1 < r_2 < \dots < r_J = R$ be a partition of $[r_1, R]$ and denote $r_0 = -r_1$. Let $\psi_{j,k}^n$ be the approximation of $\psi(r_j, \theta_k, t_n)$ and ψ^n be the solution vector at time $t = t_n$ with component $\psi_{j,k}^n$. Then the NLWE (3.1) can be discretized, for $1 \leq j < J$, $0 \leq k \leq K$ and $n = 0, 1, \dots$, as

$$\frac{\psi_{j,k}^{n+1} - 2\psi_{j,k}^n + \psi_{j,k}^{n-1}}{(\Delta t)^2} = \left(\nabla_h^2 \psi^n\right)_{j,k} + \frac{1}{\varepsilon^2} \left(V(r_j, \theta_k) - |\psi_{j,k}^n|^2\right) \psi_{j,k}^n, \tag{3.4}$$

where ∇_h^2 , the approximate differential operator for ∇^2 , is defined by [6,5,34,35]

$$\begin{aligned} \left(\nabla_h^2 \psi^n\right)_{j,k} &= \sum_{l=-K/2}^{K/2-1} \left[D_r^2(\widehat{\psi^n})_l \Big|_{r=r_j} + \frac{1}{r_j} D_r(\widehat{\psi^n})_l \Big|_{r=r_j} - \frac{l^2}{r_j^2} (\widehat{\psi_j^n})_l \right] e^{il\theta_k}, \\ D_r^2(\widehat{\psi^n})_l \Big|_{r=r_j} &= \frac{1}{\Delta r_j C_{j-1/2}} (\widehat{\psi_{j+1}^n})_l - \frac{2}{\Delta r_j \Delta r_{j-1}} (\widehat{\psi_j^n})_l + \frac{1}{\Delta r_{j-1} C_{j-1/2}} (\widehat{\psi_{j-1}^n})_l, \\ D_r(\widehat{\psi^n})_l \Big|_{r=r_j} &= \frac{\Delta r_{j-1}}{2\Delta r_j C_{j-1/2}} (\widehat{\psi_{j+1}^n})_l + \frac{\Delta r_j - \Delta r_{j-1}}{\Delta r_j \Delta r_{j-1}} (\widehat{\psi_j^n})_l - \frac{\Delta r_j}{2\Delta r_{j-1} C_{j-1/2}} (\widehat{\psi_{j-1}^n})_l; \end{aligned}$$

with $\Delta r_j = r_{j+1} - r_j$ and $C_{j-1/2} = (\Delta r_{j-1} + \Delta r_j)/2$ for $j = 0, 1, \dots, J-1$. The initial condition (3.3) is discretized as

$$\psi_{j,k}^0 = \psi_0(r_j, \theta_k), \quad \frac{\psi_{j,k}^1 - \psi_{j,k}^{-1}}{2\Delta t} = \psi_1(r_j, \theta_k), \tag{3.5}$$

$1 \leq j \leq J, 0 \leq k \leq K.$

The boundary condition (3.2) is discretized as

$$\begin{aligned} (\widehat{\psi_0^n})_l &= (-1)^l (\widehat{\psi_1^n})_l, & (\widehat{\psi_j^n})_l &= \delta_{lm}, \\ l &= -K/2, \dots, K/2-1, \end{aligned} \tag{3.6}$$

where δ_{lm} is the Kronecker delta and, for any fixed n and j , $(\widehat{\psi_j^n})_l$ ($-K/2 \leq l \leq K/2-1$) are the Fourier coefficients of the vector $\psi_{j,k}^n$ ($0 \leq k \leq K$) defined as [34,6]

$$(\widehat{\psi_j^n})_l = \frac{1}{K} \sum_{k=0}^{K-1} \psi_{j,k}^n e^{-il\theta_k}, \quad -K/2 \leq l \leq K/2-1.$$

The above discretization is spectrally accurate in the θ -direction, second order accurate in both the r -direction and

time. At each time step, the computational cost is $O(JK \ln K)$ since the fast Fourier transform (FFT) can be used in the θ -direction.

In our computation, we take $R = 7400$ for Ω_R and time step $\Delta t = 0.0001$. In the θ -direction, a uniform mesh with mesh size $\Delta\theta = \frac{\pi}{128}$, i.e. $K = 256$ in (3.4), is used. In the r -direction, a graded piecewise uniform mesh with 6001 grid points from the smallest mesh size $\Delta r = \frac{1}{60}$ for the subinterval $[0, 10]$ to the largest mesh size $\Delta r = \frac{11}{3}$ for the subinterval $[6400, 7400]$ is applied. These parameter values have been tested to assure the accuracy of the simulation results.

In all the figures presented below, we always use the symbol ‘+’ to mark the center of a vortex with index $m = +1$, either ‘-’ or ‘x’ to mark the center of a vortex with index $m = -1$, and ‘o’ to mark the collision position of two or more opposite vortices.

3.2. Stability of vortex states

In order to study the stability of vortex states of NLWE numerically, we take $\varepsilon = 1$ and $V(\mathbf{x}) \equiv 1$ in (1.1) and choose the initial data (1.2) as

$$\psi_0(\mathbf{x}) = \phi_m(\mathbf{x}), \quad \psi_1(\mathbf{x}) \equiv 0, \quad \mathbf{x} \in \mathbb{R}^2, \tag{3.7}$$

where $\phi_m(\mathbf{x})$ is given in (1.4) with $f_m(r)$ obtained numerically from (1.5) and (1.6).

As it is commonly accepted that the stability of vortices is dependent on the type of perturbations, we thus consider the stability of vortex states under a small perturbation on the initial data; an example is given by artificially setting $\psi_0(\pm 0.1, 0) = 0$.

Fig. 5 shows surface plots of $-|\psi(\mathbf{x}, t)|$ at different times for $m = 1$ and $m = 3$. From it and additional numerical experiments not shown here for brevity, we can draw the following conclusions: the vortex states with winding number $m = \pm 1$ are dynamically stable (cf. Fig. 5(a)), and resp., vortex states with winding number $|m| > 1$ are dynamically unstable in NLWE under perturbations that are either in the initial data (cf. Fig. 5(b)) or in the external potential $V(\mathbf{x})$ in (1.1). Thus, in the following sections, we only study dynamics and interaction of quantized vortices with winding numbers $m = \pm 1$ in NLWE.

4. Interaction of vortices with zero initial velocity

In this section, we report the numerical results of vortex interaction by directly simulating NLWE (1.1)–(1.3) with zero initial velocity, i.e. we take $\varepsilon = 1$ and $V(\mathbf{x}) \equiv 1$ in (1.1). The initial data is chosen as (1.8) and $\psi_1(\mathbf{x}) \equiv 0$ in (1.2).

4.1. Interactions of N ($N \geq 2$) like vortices, Patterns I & II

Fig. 6 displays contour plots of the phase S ($\psi = \sqrt{\rho} e^{iS}$) at different times when the initial data in (1.8) is chosen as (2.6) with $N = 2$, $m_0 = +1$ and $a = 2$, and Fig. 7 shows time evolution of the vortex centers for different $N \geq 2$ in Pattern I. In addition, Figs. 8 and 9 show similar results when the initial data in (1.8) is chosen as (2.15)–(2.16) with $m_0 = +1$, i.e. Pattern II.

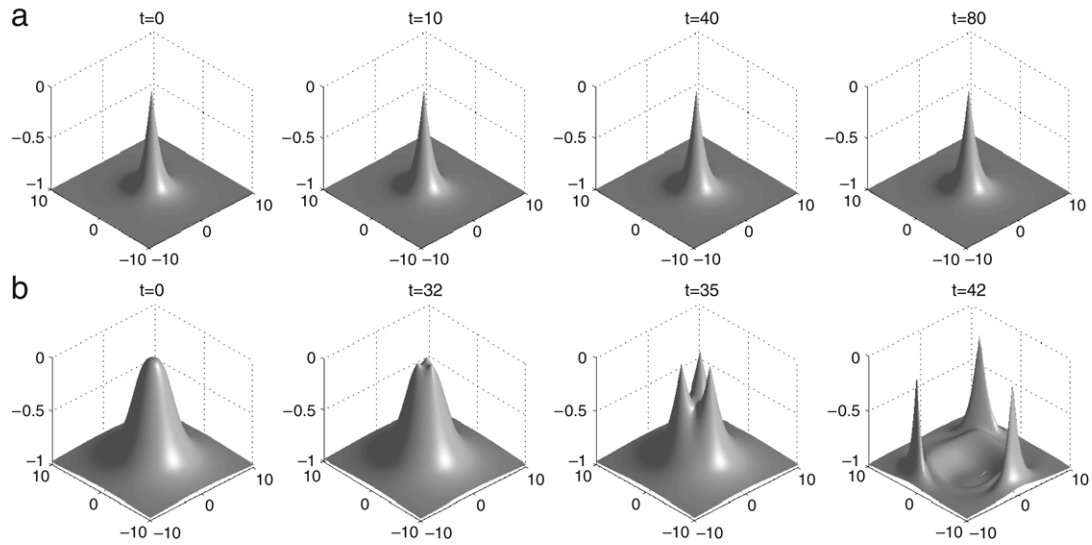


Fig. 5. Surface plots of $-\lvert\psi(x, t)\rvert$ at different times for the stability study of the vortex states in NLWE under a perturbation on the initial data for different winding numbers: (a) $m = 1$, and (b) $m = 3$.

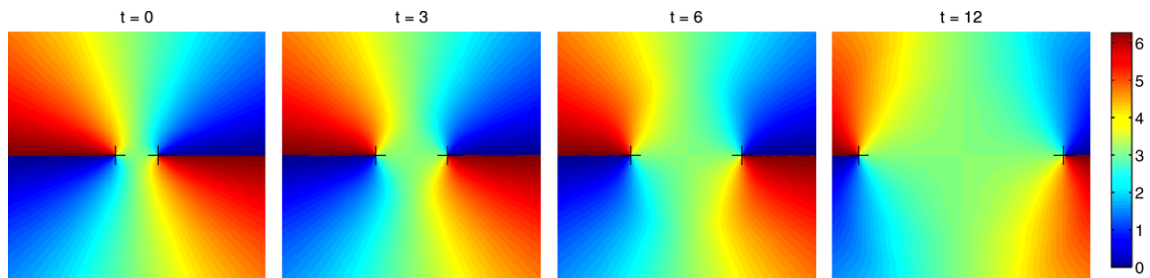


Fig. 6. Contour plots of the phase $S (\psi = \sqrt{\rho} e^{iS})$ at different times when the initial data is chosen as Pattern I with $N = 2, m_0 = +1$ and $a = 2$ in (2.6).

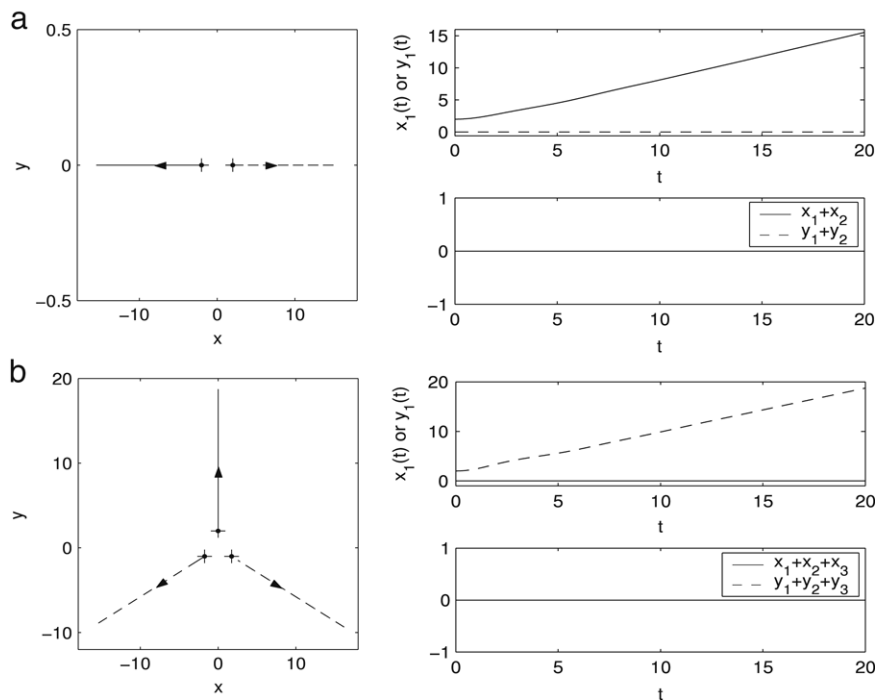


Fig. 7. Time evolution of vortex centers when the initial data is chosen as Pattern I with $m_0 = +1$ and $a = 2$ in (2.6) for different N : (a) $N = 2$, and (b) $N = 3$.

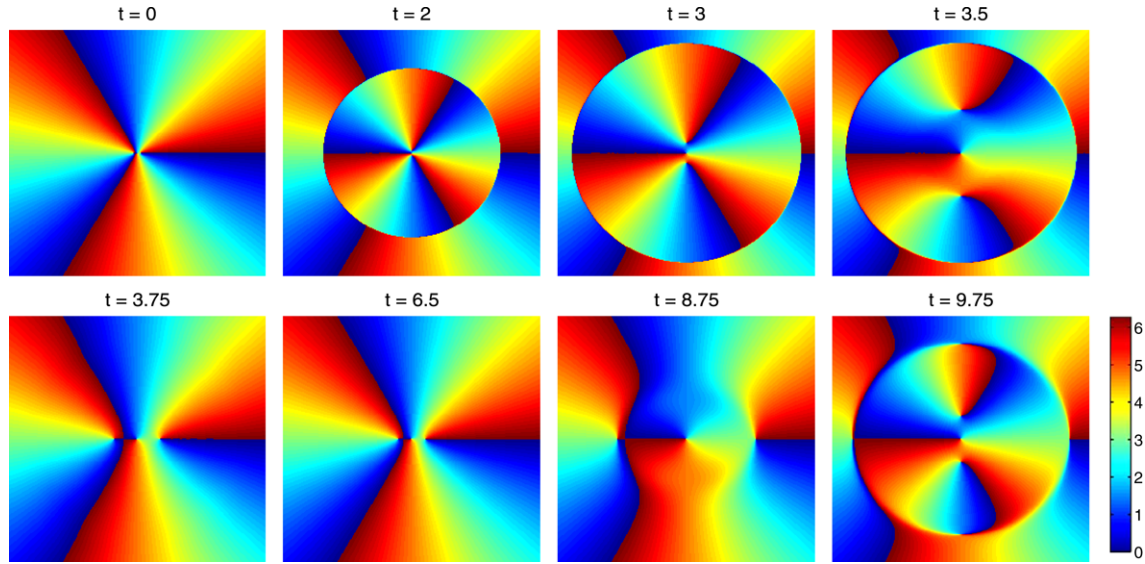


Fig. 8. Contour plots of the phase S at different times for the interaction of three like vortices in Pattern II with $N = 3$, $m_0 = +1$ and $a = 0.1$ in (2.15)–(2.16).

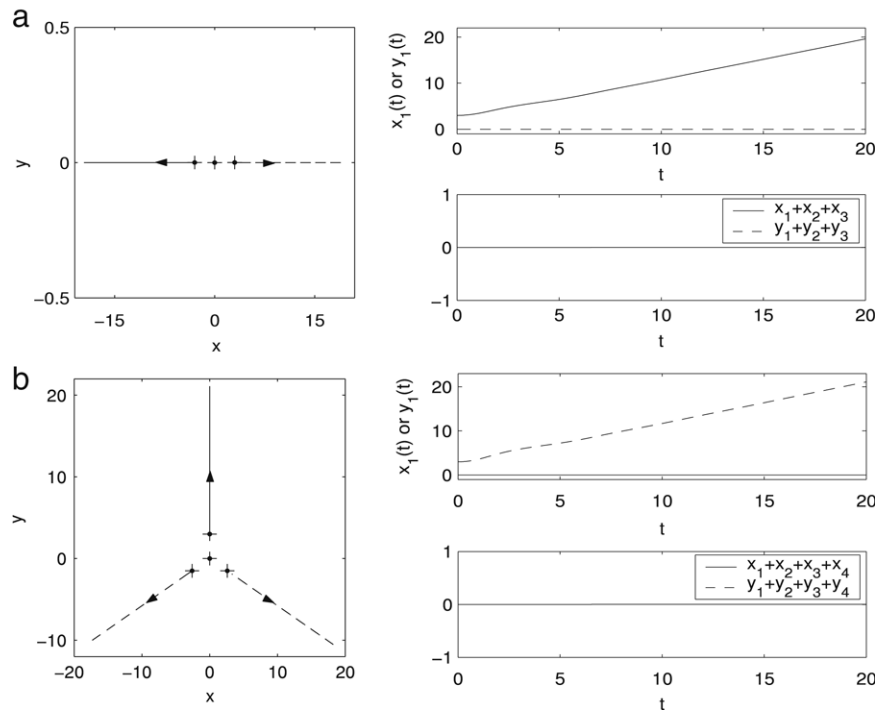


Fig. 9. Time evolution of vortex centers when the initial data is chosen as Pattern II with $m_0 = +1$ and $a = 3$ in (2.15)–(2.16) for different N : (a) $N = 3$, and (b) $N = 4$.

From Figs. 6–9 and additional numerical experiments not shown here for brevity, we can draw the following conclusions for the interaction of N like vortices when the initial data is chosen as either Pattern I or II:

(i) The mass center of the vortex centers is conserved for any time $t \geq 0$ (cf. Figs. 7 and 9), which confirms the conservation law in (2.3).

(ii) Vortices with the same index undergo a repulsive interaction and they never collide (cf. Figs. 6, 7 and 9) when they are well-separated. In Pattern II, the vortex initially at the

origin does not move during the dynamics (cf. Fig. 9), which confirms the analytical solution (2.17).

(iii) Due to the symmetry of the initial data, each vortex of those initially located on a circle moves along the line passing through its initial location and the origin, and at any time $t \geq 0$, their centers are always on a circle (cf. Figs. 6–9) when they are well-separated, which confirms the analytical solutions (2.7) and (2.18).

(iv) When the distance between the vortex centers is very small at $t = 0$, i.e. they are overlapped, complicated interaction

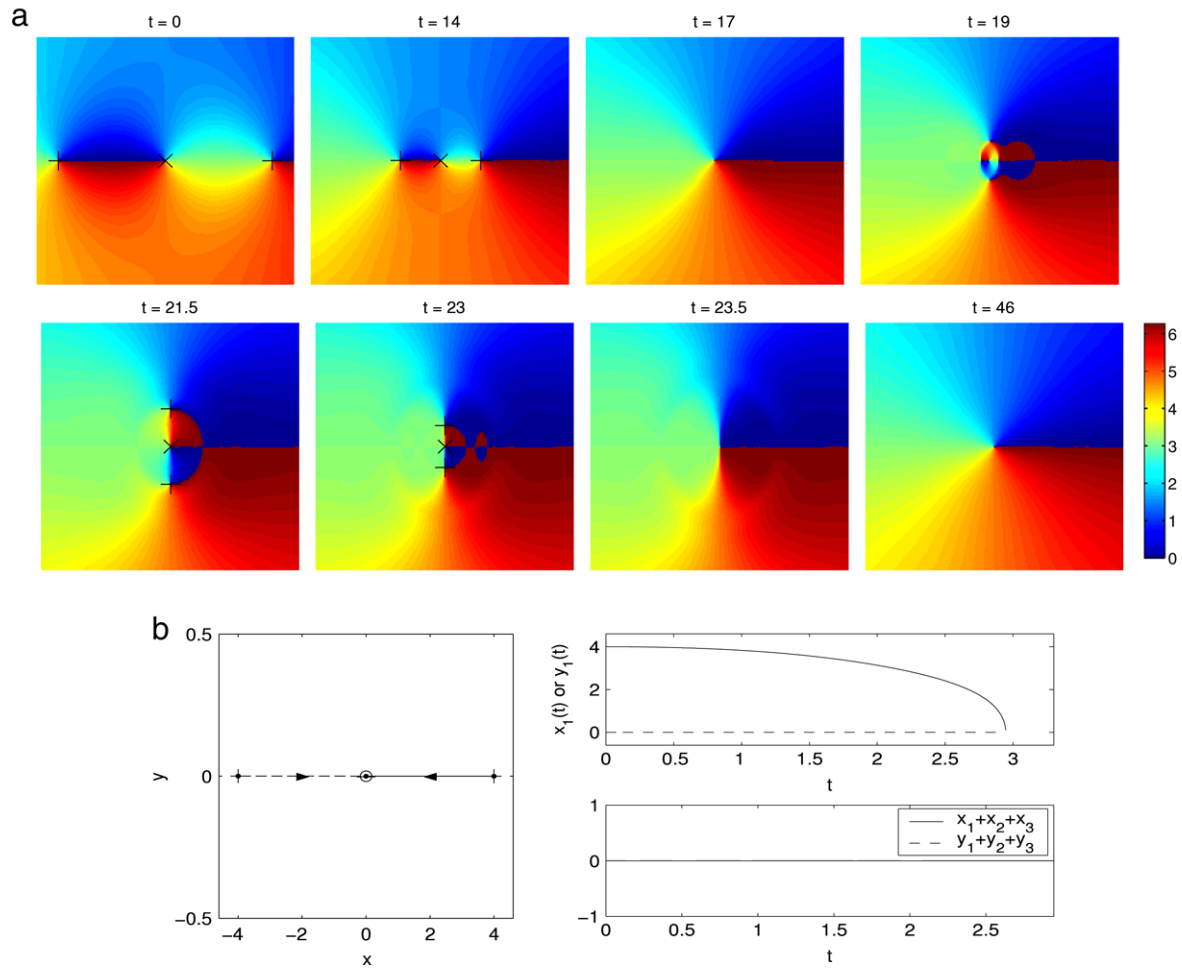


Fig. 10. Dynamics of three opposite vortices when the initial data is chosen as Pattern III with $N = 3$ and $m_0 = +1$ in (2.15)–(2.16) for different a : (a) Contour plots of the phase S at different times when $a = 10 \gg 1$, and (b) Time evolution of vortex centers when $a = 4 = O(1)$.

patterns of the vortex centers of the NLWE are observed in our direct numerical results (cf. Fig. 8).

(v) There exists a critical time $t_{cr} > 0$ dependent of N and a , such that when $0 \leq t \leq t_{cr} = O(1)$, the vortices initially located on a circle move with a varying velocity, and after time t_{cr} , i.e. for $t \geq t_{cr}$, their velocity is almost a constant (cf. Figs. 7 and 9).

(vi) In Patterns I and II, if the initial distance between vortex centers is large, i.e. they are well-separated, the solutions of the reduced dynamic laws agree with our numerical results of NLWE qualitatively, and quantitatively with a proper κ chosen in (1.9), which depends on the initial setup in (1.8); while when the initial distance is small, i.e. they are overlapped, the solutions of the reduced dynamic laws do not agree with our numerical results of NLWE qualitatively (cf. Fig. 8) and corrections, e.g. the correction term denoting the residuals of a holomorphic function defined away from the vortices in [22], need to be added to the reduced dynamic laws.

4.2. Interactions of N ($N \geq 3$) opposite vortices, Pattern III

Fig. 10 shows contour plots of the phase S and time evolution of the vortex centers when the initial data in (1.8) is

chosen as Pattern III with $m_0 = +1$ and $N = 3$ in (2.15) and (2.16) for different a . Figs. 11 and 12 display similar results for $N = 4$ and $N = 5$, respectively.

From Figs. 10 to 12 and additional numerical experiments not shown here for brevity, we can draw the following conclusions for the interaction of N opposite vortices when the initial data is chosen as Pattern III:

(i) The mass center of the vortex centers is conserved for any time $t \geq 0$, which again confirms the conservation law in (2.3).

(ii) The vortex initially at the origin does not move for any time $t \geq 0$ (cf. Figs. 10(b), 11(b), 12(a) and (b)), which confirms the analytical solution (2.23). After a short time period, each vortex of those initially located on a circle moves to the origin when $N = 3$, and resp. moves away when $N \geq 5$, along the line passing through its initial location and the origin, and the vortex centers are always on a circle (cf. Figs. 10(b), 11(b), 12(a) and (b)).

(iii) When $N = 3$, collisions between the three vortex centers are observed at a critical time t_c (cf. Fig. 10) and this collision time is almost linearly proportional to the initial distance a when $a \gg 1$. At time $t = t_c$ they collide at the origin, and after it only one vortex with index $m = m_0$ is left

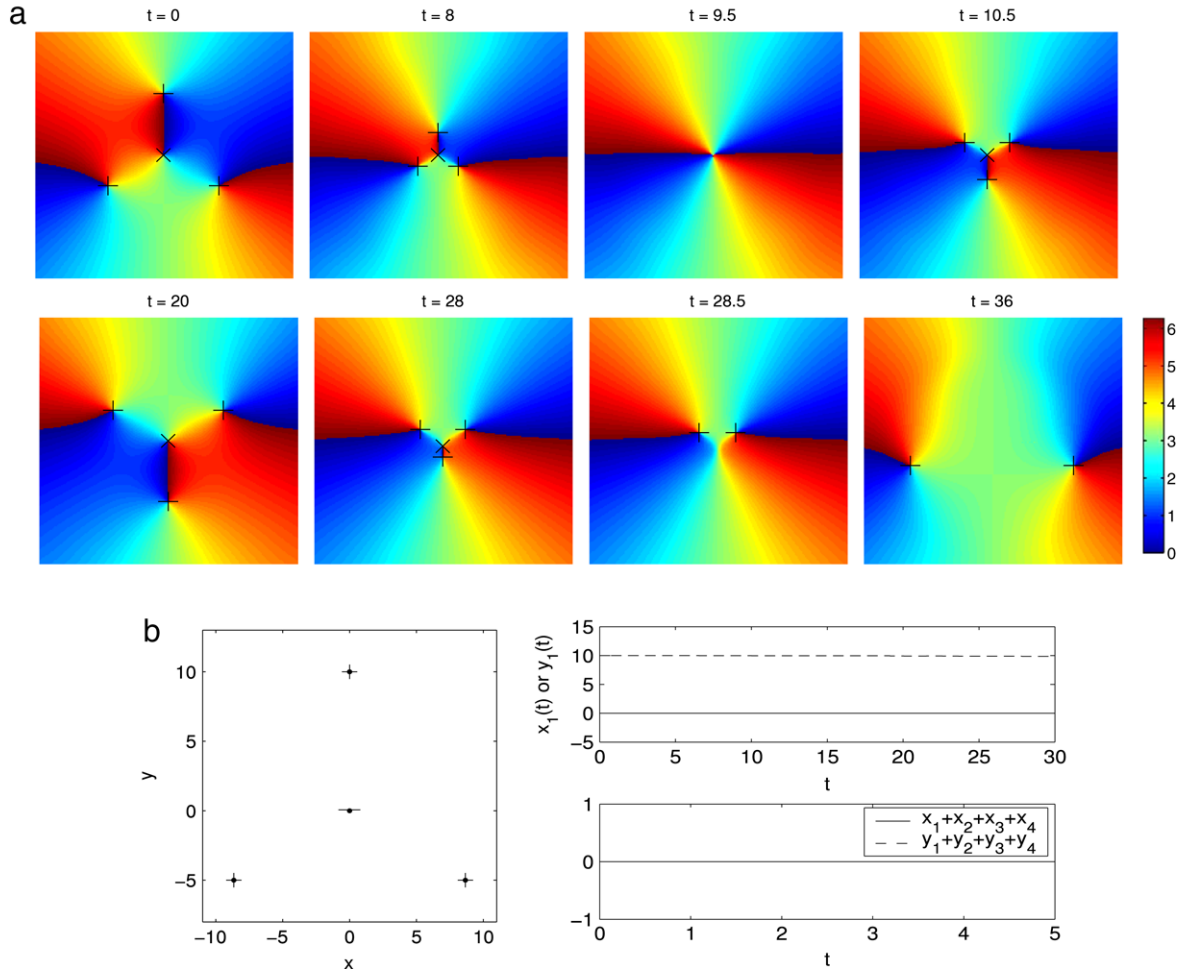


Fig. 11. Dynamics of four opposite vortices when the initial data is chosen as Pattern III with $N = 4$ and $m_0 = +1$ in (2.15)–(2.16) for different a : (a) Contour plots of the phase S at different times when $a = 4 = O(1)$, and (b) Time evolution of vortex centers when $a = 10 \gg 1$.

and it stays at the origin for any time $t \geq t_c$ (cf. Fig. 10). For the collision pattern, there exists a critical $a_{cr} = O(1)$. When $0 < a < a_{cr}$, the interaction is always attractive and the three vortices collide at the origin when they meet each other at the first time (cf. Fig. 10(b)). On the other hand, when $a > a_{cr}$, the three vortices first undergo an attractive interaction towards the origin but they don't collide when they meet at the origin the first time (cf. Fig. 10(a) with $t = 17$). The three vortices interact and the two vortices with winding number $m = +1$ penetrate the origin and move first outwards (repulsive interaction) due to nonzero velocity and then towards (attractive interaction) the origin along the line perpendicular to that connecting the original three vortex centers (cf. Fig. 10(a)). Eventually, they collide at the origin when they meet each other the second time.

(iv) When $N = 4$, if a is very large, the four opposite vortices would stay at their initial locations for a long time period (cf. Fig. 11(b)) and the larger is the initial distance a , the longer is the time period. On the other hand, if a is small, they first undergo attractive interactions towards the origin and they don't collide when they meet at the origin the first time (cf. Fig. 11(a) with $t = 9.5$). The four vortices interact and the three

vortices with winding number $m = +1$ penetrate the origin and move first outwards from the origin (repulsive interactions) due to nonzero velocity and then towards to the origin (attractive interactions) and finally collide there (cf. Fig. 11(a)). After the collision, there are two like vortices left and they undergo a repulsive interaction (cf. Fig. 11(a) with $t \geq 28.5$).

(v) When $N \geq 5$, for large a , the vortices undergo repulsive interactions and they never collide (cf. Fig. 12(b)), while for small a , the vortices first undergo attractive interactions within time $0 \leq t \leq t_0$ but they don't collide, and after time t_0 , their interactions become repulsive (cf. Fig. 12(a)).

(vi) In Pattern III, the solutions of the reduced dynamic laws agree with our numerical results of NLWE qualitatively when the distances between the vortex centers are very large, i.e. when they are well-separated. On the contrary, they are completely different when the distances are small, i.e. when they are overlapped (c.f. Figs. 11(a) and 10(a) for $t \geq 17$)! One may argue that when the distance between the vortex centers is small, the cores of the vortices are overlapped and thus the next order effect becomes important in the underlying vortex motion of the original NLWE. In this regime, correction must be added, e.g. the correction term denoting the residuals of a holomorphic

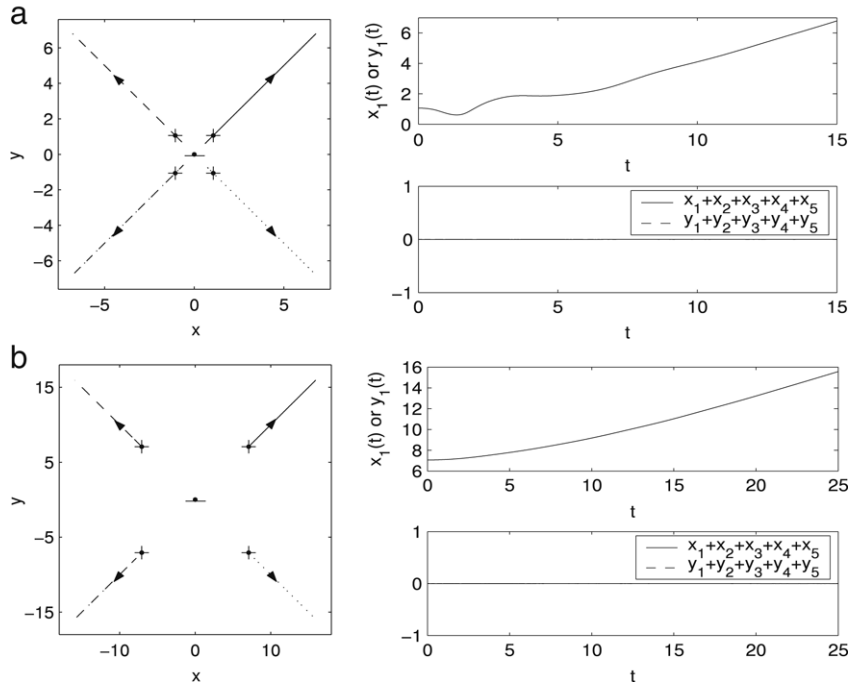


Fig. 12. Time evolution of vortex centers when the initial data is chosen as Pattern III with $N = 5$ and $m_0 = +1$ in (2.15)–(2.16) for different a : (a) $a = 1 = O(1)$, and (b) $a = 7 \gg 1$.

function defined away from the vortices in [22], to the reduced dynamic laws.

4.3. Interactions of two opposite vortices, Pattern IV

Fig. 13 displays contour plots of the phase S and time evolution of the two vortex centers when the initial data in (1.8) is chosen as Pattern IV with $m_0 = +1$ and $a = 2$ in (2.27). In addition, Fig. 14 shows the collision time t_c vs the initial distance between the two vortex centers.

From Figs. 13 and 14, we can draw the following conclusions for the interaction of two opposite vortices when the initial data is chosen as Pattern IV:

(i) The mass center of the two vortex centers is conserved (cf. Fig. 13(b)), which again confirms the conservation law in (2.3).

(ii) Two vortices with opposite indices undergo an attractive interaction, and their centers move along a straight line passing through their locations at $t = 0$. The speed of the motion for the two vortex centers depends on their distance. The smaller is the distance, the faster is the motion (cf. Fig. 13).

(iii) There exists a critical time $t_c > 0$, and at time $t = t_c$ the two opposite vortices collide with each other at the origin (cf. Fig. 13). From our numerical results, we find numerically that the collision time depends on the distance of the two vortex centers at $t = 0$ as (cf. Fig. 14)

$$t_c = O(a), \quad a \gg 1, \tag{4.1}$$

which confirms the result (2.31) of the reduced dynamic laws.

(iv) Again, in Pattern IV, the solutions of the reduced dynamic laws agree with our numerical results of NLWE

qualitatively, and quantitatively if a proper κ in (1.9) is chosen, which depends on the initial setup in (1.8).

4.4. Interactions of vortices with nonsymmetric setups

In this subsection, we report the interaction of quantized vortices in NLWE with nonsymmetric initial setups. For simplicity, we only consider the case of three vortices, i.e. $N = 3$. Here we consider the following three different cases (with $m_1 = m_3 = +1$ in all the cases):

Case 1. $\mathbf{x}_1^0 = (-a, -b/2), \quad \mathbf{x}_2^0 = (0, b),$

$\mathbf{x}_3^0 = (a, -b/2), \quad m_2 = +1;$

Case 2. $\mathbf{x}_1^0 = (-\sqrt{3}a/2, -a/2), \quad \mathbf{x}_2^0 = (0, a),$

$\mathbf{x}_3^0 = (\sqrt{3}a/2, -a/2), \quad m_2 = -1;$

Case 3. $\mathbf{x}_1^0 = (-a, -b/2), \quad \mathbf{x}_2^0 = (0, b),$

$\mathbf{x}_3^0 = (a, -b/2), \quad m_2 = -1.$

Fig. 15 shows time evolution of the vortex centers of the NLWE (1.1) when the initial data in (1.8) is chosen as Case 1. For comparison, we also plot the numerical solutions of the reduced dynamic laws (1.9) by using the standard finite difference discretization for the second order ODEs (1.9) with the initial data in (1.10) is chosen as in Case 1. In addition, Figs. 16 and 17 show similar results for Case 2 and Case 3, respectively.

Based on Figs. 18–20 and our additional numerical results not shown here for brevity, we can draw the following conclusions for the interactions of three vortices with nonsymmetric initial setups:

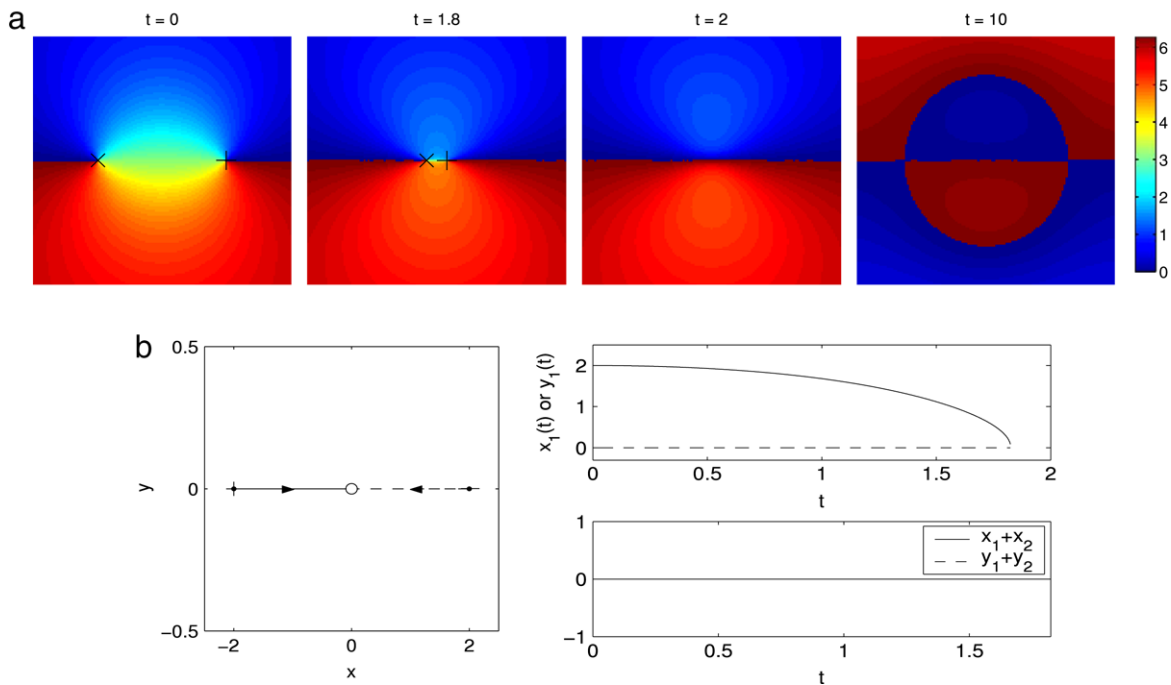


Fig. 13. Dynamics of two opposite vortices when the initial data is chosen as Pattern IV with $m_0 = +1$ and $a = 2$ in (2.27): (a) Contour plots of the phase S at different times, and (b) Time evolution of vortex centers.

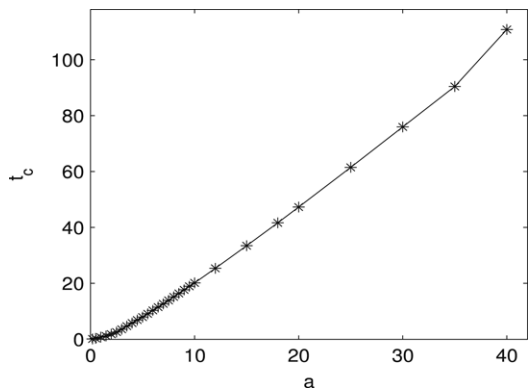


Fig. 14. The collision time t_c vs initial setup a in Pattern IV.

(i) The mass centers of the vortex centers are not conserved (cf. Figs. 15(a) and (c), 16(a) and (c), 17(a) and (c)) during the dynamics within the time frame we computed the solutions, which conflicts with the results from the reduced dynamic law (cf. Figs. 15(b) and (d), 16(b) and (d), 17(b) and (d)). These suggest that the reduced dynamic law (1.9)–(1.10) has considerable discrepancy with the original dynamics in some regimes. One may argue that a possible cause is due to the fact that the reduced dynamic law is the adiabatic approximation in the leading order when the N vortices are well-separated, and thus the next order effect becomes important in the underlying vortex motion of the original NLWE when the N vortices are not well-separated.

(ii) For the interaction of three like vortices, the three vortex centers move almost on three straight lines after some time t_0 , and they never collide (cf. Fig. 15). On the contrary, for the interaction of three opposite vortices, our numerical results by directly simulating NLWE (1.1)–(1.3) show that they will

collide at finite time and after collision, only one vortex is left (cf. Figs. 16(a) and (c), 17(a) and (c)); however, the solutions of the reduced dynamic law indicate that these three vortices undergo a periodic interaction with a period depending on the initial distance between them (cf. Figs. 16(b) and (d), 17(b) and (d)), and they never collide!

(iii) For the interaction of vortices with nonsymmetric initial setup, the solutions of the reduced dynamic laws agree with our numerical results of NLWE qualitatively if they have the same winding number and they are well-separated; on the contrary, if they are not well-separated or they have different winding numbers, the solutions of the reduced dynamic laws and NLWE may be completely different!

5. Other dynamics of vortices

In this section, we report the numerical results of the vortex dynamics of NLWE with either nonzero initial velocity or inhomogeneous external potential by directly simulating NLWE (1.1)–(1.3).

5.1. Vortex interactions with nonzero initial velocity

For simplicity, here we only report interactions of two like and opposite vortices, and we take $\varepsilon = 1$ and $V(\mathbf{x}) \equiv 1$ in (1.1). The initial data $\psi_0(\mathbf{x})$ in (1.2) is chosen as (1.8) with $N = 2$. We take $\psi_1(\mathbf{x})$ in (1.2) as

$$\partial_t \psi(\mathbf{x}, 0) = \psi_1(\mathbf{x}) = \alpha e^{-(x^2+y^2)/16}, \quad \mathbf{x} \in \mathbb{R}^2, \quad (5.1)$$

where the parameter $\alpha = \pm 1$, that is, we consider two types of initial velocities which have the same magnitudes but different directions at the point $\mathbf{x} \in \mathbb{R}^2$.

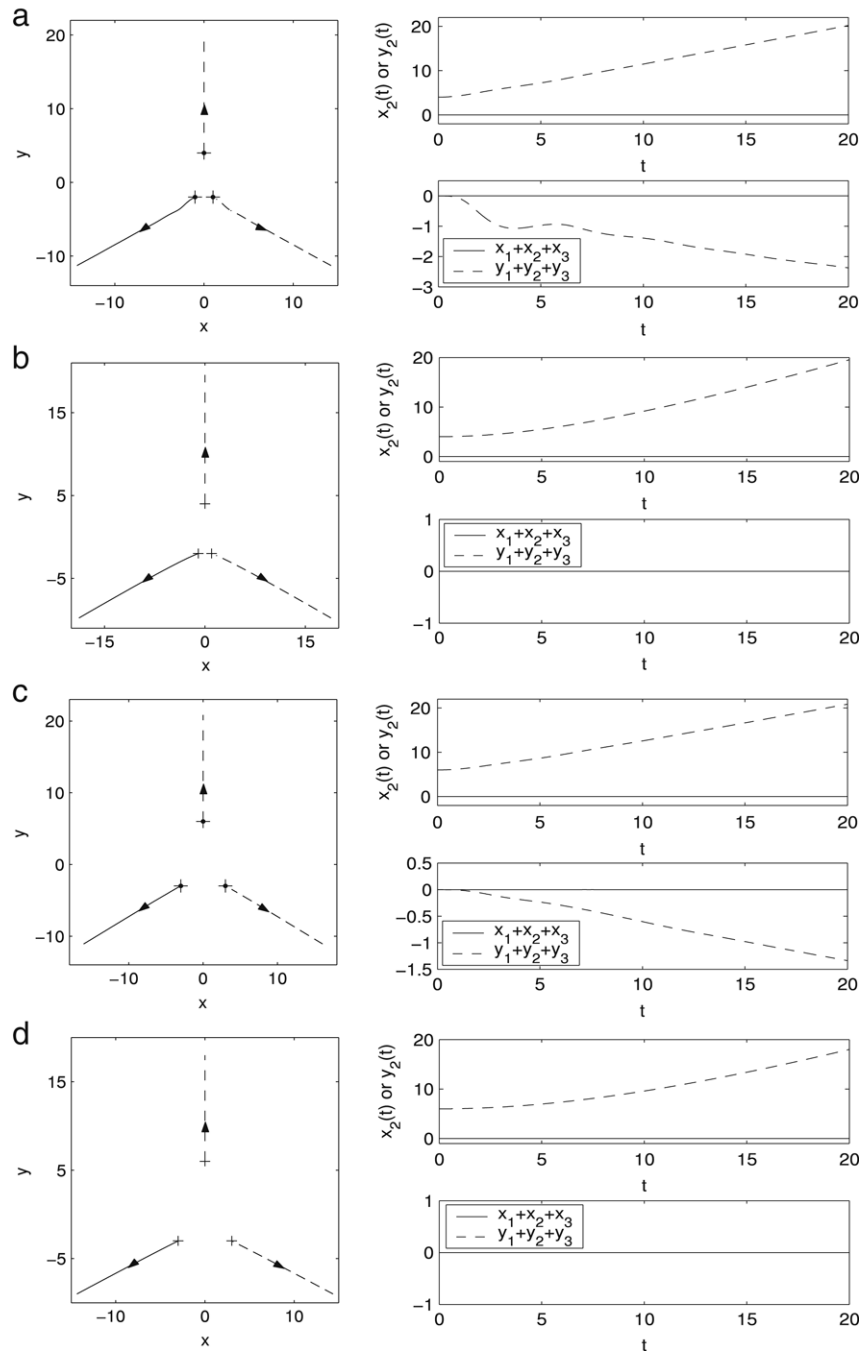


Fig. 15. Time evolution of vortex centers when the initial data in (1.8) is chosen as Case 1 for different initial distances between the vortex centers: (a) and (b) $a = 1, b = 4$, and (c) and (d). $a = 3, b = 6$; where (a) and (c): from directly simulating NLWE (1.1)–(1.3), and (b) and (d): from reduced dynamic law (1.9)–(1.10).

Figs. 18 and 19 show the interaction of two like and opposite vortices in the NLWE (1.1) with nonzero initial velocity chosen as (5.1) with $\alpha = 1$, respectively. In addition, Figs. 20 and 21 show similar results for $\alpha = -1$ in (5.1).

Based on Figs. 18–21 and our additional numerical results not shown here for brevity, we can draw the following conclusions for the interactions of two vortices in the NLWE (1.1) under nonzero initial velocity:

(i) Two like vortices may undergo repulsive interaction and attractive interaction depending on the initial velocity.

But they never collide with each other. In fact, for the two like vortices, if $\alpha = +1$ in (5.1) and a is small, the two vortices first undergo an attractive interaction towards the origin due to the nonzero initial velocities at $\mathbf{x} = (\pm a, 0)^T$, e.g. $\psi_1(\mathbf{x}, 0) \approx 0.8688$ when $a = 1.5$, and then they meet at the origin, reflect each other to the y -axis and undergo a repulsive interaction (cf. Fig. 18(a)); while when a is large, the two vortices have a repulsive interaction which is similar to the case with zero initial velocity (cf. Fig. 18(b)). If $\alpha = -1$ in (5.1),

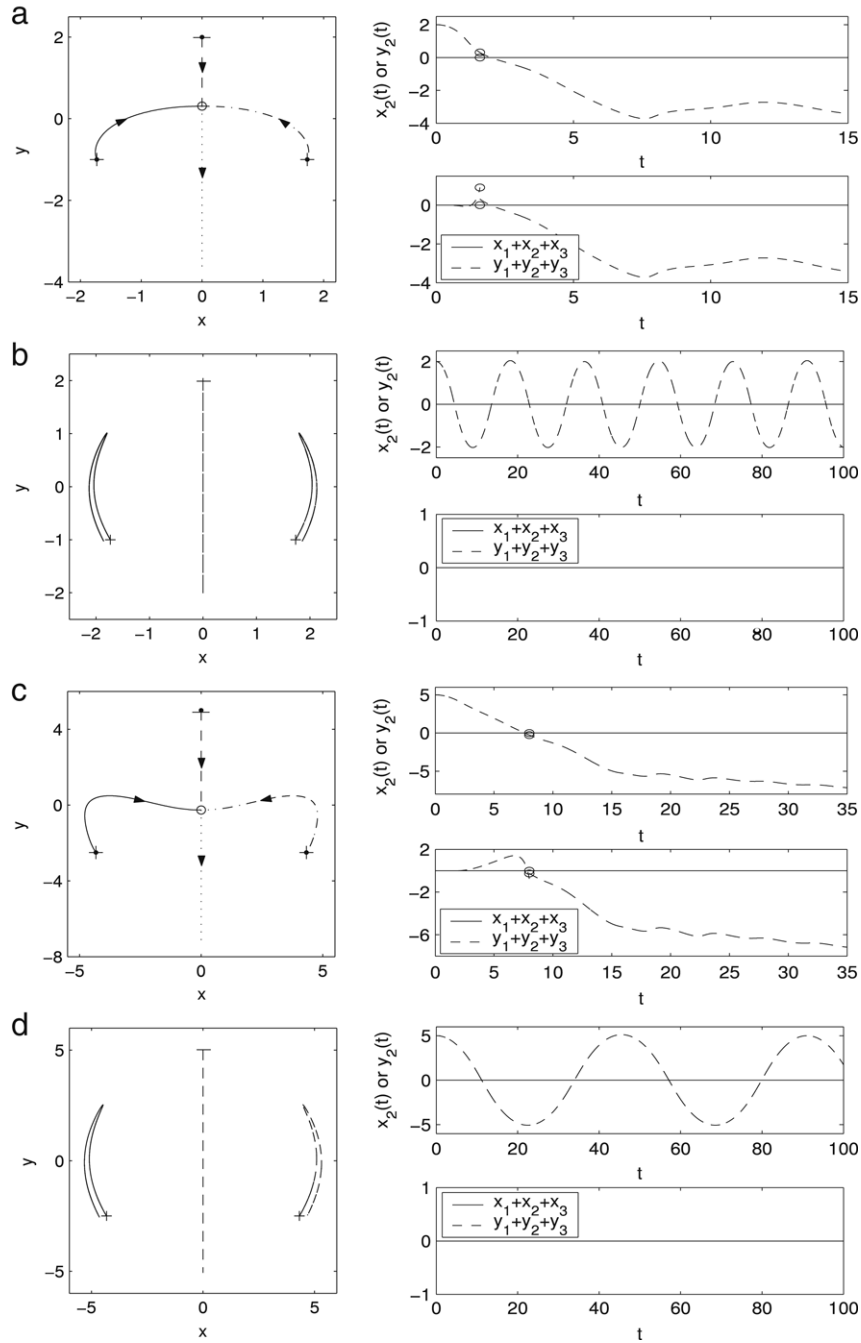


Fig. 16. Time evolution of vortex centers when the initial data in (1.8) is chosen as Case 2 for different initial distances between the vortex centers: (a) and (b) $a = 2$, and (c) and (d). $a = 5$; where (a) and (c): from directly simulating NLWE (1.1)–(1.3), and (b) and (d): from reduced dynamic law (1.9)–(1.10).

the two like vortices always undergo a repulsive interaction (cf. Fig. 20).

(ii) Two opposite vortices may undergo repulsive interaction and attractive interaction depending on the initial velocity. They will collide with each other at finite time. After the collision, they will disappear together. In fact, for the two opposite vortices, if $\alpha = +1$ in (5.1) and the initial distance a is small or intermediate, e.g. when $a = 0.5$ is small, at $t = t_c = O(a)$ they collide and annihilate at the origin, after some time there are two new opposite vortices generated and they first undergo

a repulsive interaction and then an attractive interaction, and eventually they collide at the origin and no vortex exists after it (cf. Fig. 19(a)); and when $a = 8$ is intermediate, at $t = t_c \approx 1.4$ another two opposite vortices are generated near the origin and then the two pairs of opposite vortices attract each other and collide at two different locations (cf. Fig. 19(b)). On the contrary, when $\alpha = -1$ in (5.1) and the initial distance is small or intermediate, the two opposite vortices first undergo a repulsive interaction and then an attractive interaction, and eventually they collide at the origin (cf. Fig. 21(a)). In addition,

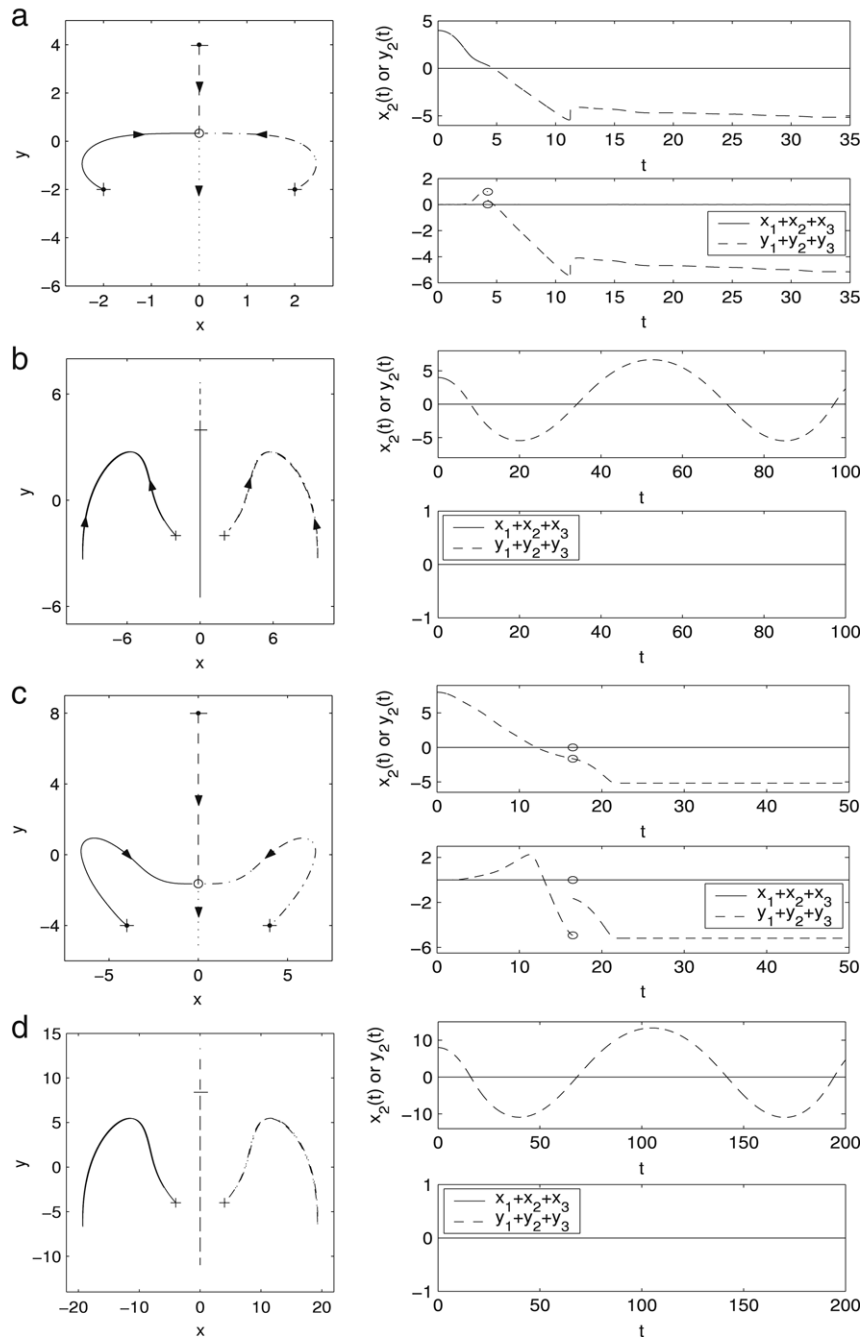


Fig. 17. Time evolution of vortex centers when the initial data in (1.8) is chosen as Case 3 for different initial distances between the vortex centers: (a) and (b) $a = 2$, $b = 4$, and (c) and (d). $a = 4$, $b = 8$; where (a) and (c): from directly simulating NLWE (1.9)–(1.10), and (b) and (d): from reduced dynamic law (1.9)–(1.10).

when a is extremely large in this case, e.g. $a > 30$, the interactions are always similar to those with zero initial velocity (cf. Figs. 19(c) and 21(b)) no matter $\alpha = +1$ or -1 in (5.1), which is because $|\psi_1(\mathbf{x}, 0)| \approx 0$ when $\mathbf{x} = (\pm a, 0)^T$ and a is large.

(iii) In general, the interaction patterns of two vortices in the NLWE (1.1) under nonzero initial velocity, i.e. $\psi_1 \neq 0$ in (1.2), are much more complicated than those under zero initial velocity. The larger is the initial velocity, the stronger is the effect on the interaction patterns.

(iv) In general, it is not easy to determine explicitly the initial velocity in (1.10) for the reduced dynamic laws (1.9) from the nonzero initial velocity in (1.2) for the NLWE (1.1). The reduced dynamic laws for the NLWE with nonzero initial velocity may exist, but they are usually not available explicitly!

5.2. Vortex dynamics under an inhomogeneous potential

Here we also numerically study the dynamics of vortices under an inhomogeneous external potential. We take $V(\mathbf{x})$ in

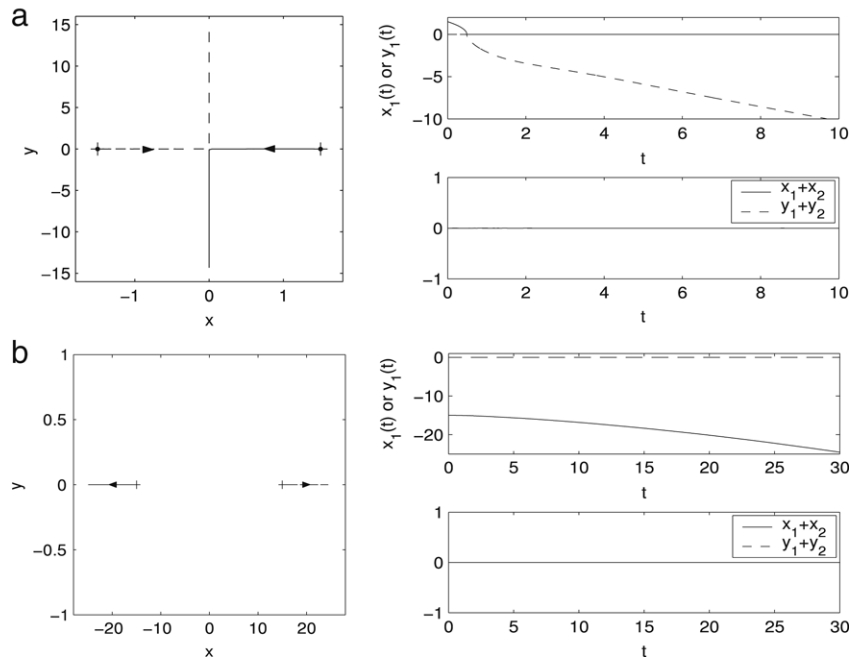


Fig. 18. Time evolution of vortex centers for the interaction of two like vortices in the NLWE (1.1) with nonzero initial velocity chosen as (5.1) with $\alpha = +1$ for different initial distance a : (a) $a = 1.5$; (b) $a = 15$.

(1.1) as

$$V(\mathbf{x}) = \frac{\frac{1}{2} + \gamma_x x^2 + \gamma_y y^2}{1 + \gamma_x x^2 + \gamma_y y^2} = 1 - \frac{1}{2(1 + \gamma_x x^2 + \gamma_y y^2)},$$

$$\mathbf{x} \in \mathbb{R}^2 \tag{5.2}$$

with γ_x and γ_y two positive constants. It is easy to see that $V(\mathbf{x})$ attains its minimum value $\frac{1}{2}$ at the origin. The initial data in (1.2) is chosen as

$$\psi(\mathbf{x}, 0) = \psi_0(\mathbf{x}) = \phi_1(\mathbf{x} - \mathbf{x}^0), \quad \psi_1(\mathbf{x}) \equiv 0,$$

$$\mathbf{x} \in \mathbb{R}^2, \tag{5.3}$$

where $\phi_1(\mathbf{x})$ is the vortex state of (1.4) with winding number $m = 1$ and \mathbf{x}^0 is a given point.

Figs. 22 and 23 display time evolution of the vortex centers for symmetric and anisotropic inhomogeneous external potential, respectively.

From Figs. 22 and 23, we can draw the following conclusions: (i) For both cases, the vortex center moves towards the position where the external potential attains its minimum value. The speed of the motion depends on the values of the parameter ε . (ii) If $\gamma_x = \gamma_y = 1$, the trajectory for different ε is the same, and it is a straight line connecting the initial location of the vortex center and the origin. After reaching the origin, the vortex will oscillate with respect to the origin along the straight line due to nonzero velocity (cf. Fig. 22). (iii) For an anisotropic potential, e.g. $\gamma_x = 1$ and $\gamma_y = 5$, the trajectory of the vortex center depends on the parameter ε (cf. Fig. 23(a)). Rigorous justification, e.g. reduced dynamic laws for NLWE with inhomogeneous external potential, for this observation is still not available.

6. Conclusion

We have studied the dynamics and interaction of quantized vortices in the nonlinear wave equation (NLWE) both analytically and numerically. From the analytical perspective, we reviewed the second order nonlinear ordinary differential equations of the reduced dynamic laws governing the dynamics of N vortex centers; proved that the mean velocity of the vortex centers is conserved and the mass center of the vortex centers is conserved if the initial mean velocity is zero based on the reduced dynamic laws; and solved analytically the nonlinear ordinary equations (ODEs) of the reduced dynamic laws with a few types of initial data. These conservation quantities and analytical solutions of the reduced dynamic laws provide qualitative and quantitative interaction patterns of quantized vortices in the NLWE when they are well-separated. From the numerical perspective, we introduced an efficient and accurate Fourier pseudospectral method based on using the polar coordinate to match the highly oscillating nonzero far field condition for solving the NLWE, and applied it to numerically study issues such as the stability of vortex states in the NLWE, the interaction of a few vortices with different initial data and motion of a vortex under an inhomogeneous external potential. We found numerically that quantized vortices with winding number $m = \pm 1$ are dynamically stable, and resp., $|m| > 1$ are dynamically unstable, in the dynamics of the NLWE. Comparisons between the solutions of the reduced dynamic laws and direct simulation results of the NLWE were provided. Some conclusive findings were obtained, and discussions on numerical and theoretical results were made

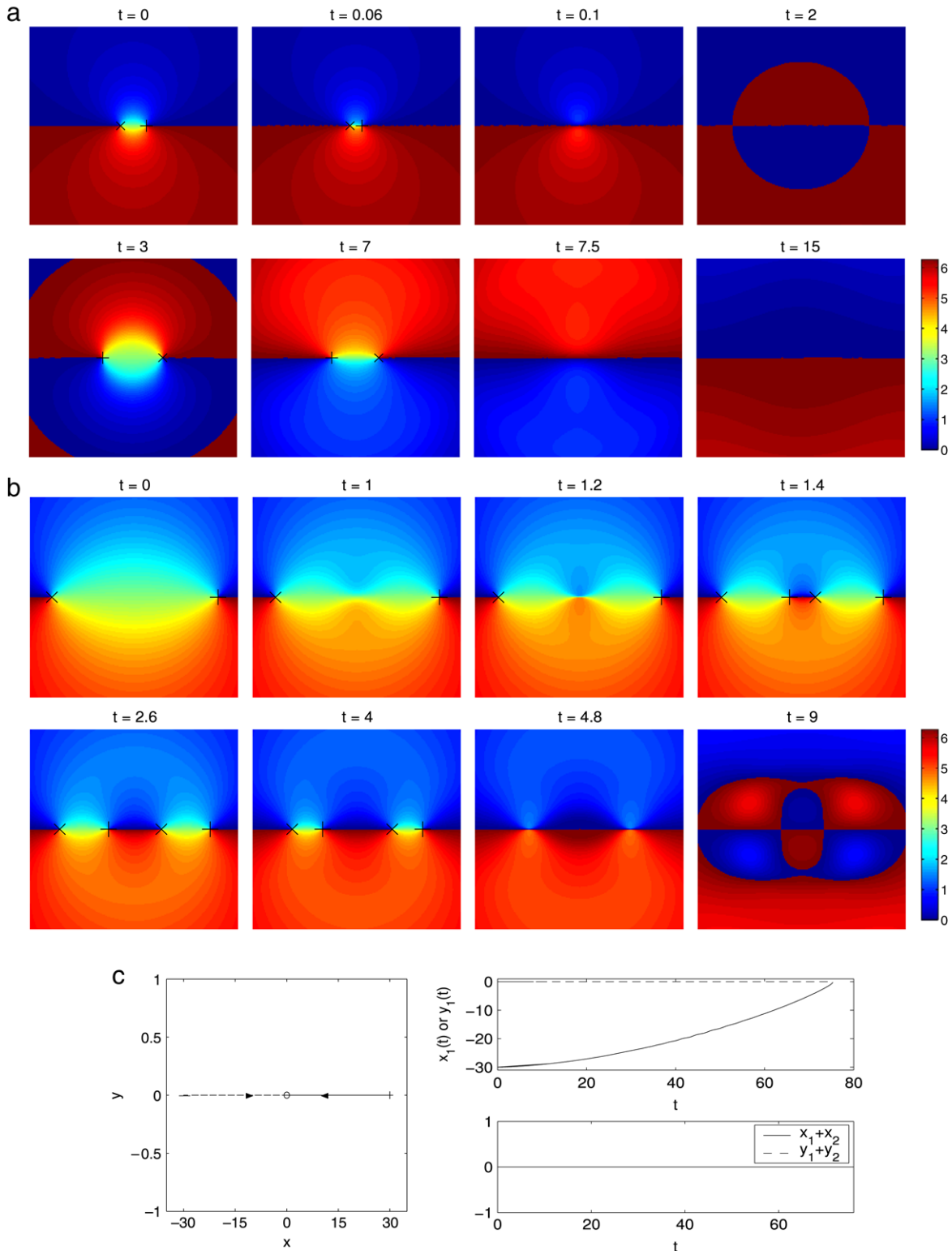


Fig. 19. Interaction of two opposite vortices in the NLWE (1.1) with nonzero initial velocity chosen as (5.1) with $\alpha = +1$ for different initial distance a : (a) Contour plots of the phase S with $a = 0.5$; (b) Contour plots of the phase S with $a = 8$; and (c) Time evolution of the two vortex centers with $a = 30$.

to provide further understanding of vortex interactions in the NLWE. In fact, the analytical and numerical results in the paper enhanced significantly our understanding on the stability and interaction of quantized vortices in the nonlinear wave equation.

Acknowledgments

We acknowledge support from the Ministry of Education of Singapore grant No. R-146-000-083-112. The authors thank the referees for their valuable comments to improve the paper. W.B.

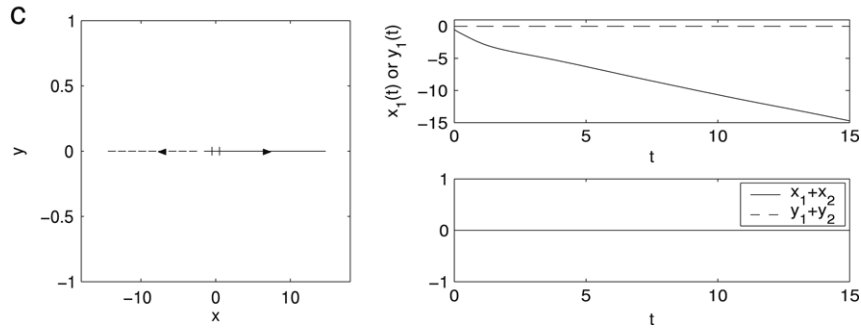


Fig. 20. Time evolution of vortex centers for the interaction of two like vortices in the NLWE (1.1) with nonzero initial velocity chosen as (5.1) with $\alpha = -1$ and initial distance $a = 0.5$.

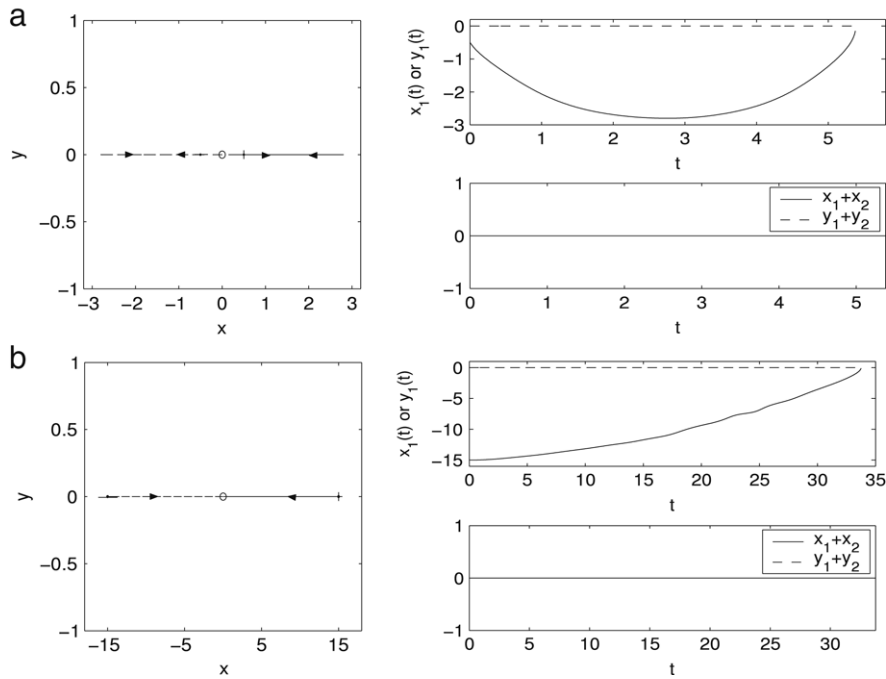


Fig. 21. Time evolution of vortex centers for the interaction of two opposite vortices in the NLWE (1.1) with nonzero initial velocity chosen as (5.1) with $\alpha = -1$ and different initial distance a : (a) $a = 0.5$; (b) $a = 15$.

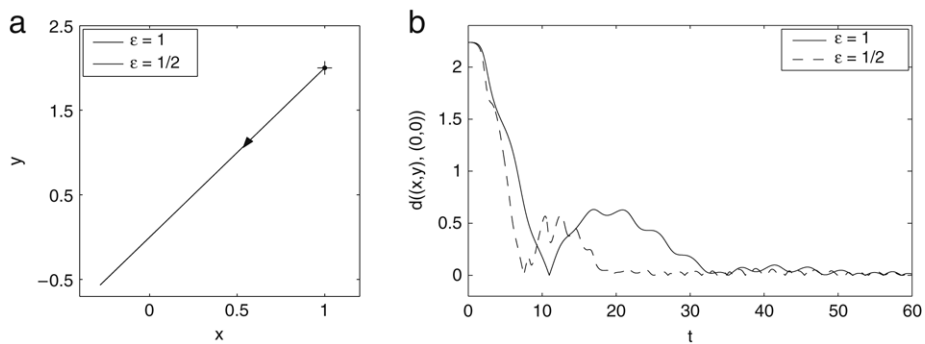


Fig. 22. Time evolution of the vortex center under a symmetric inhomogeneous external potential (5.2) with $\gamma_x = \gamma_y = 1$. (a) trajectories for different ϵ , and (b) distance between the vortex center and the origin.

thanks Professor Jack X. Xin for helpful discussions on the subject. This work was partially done while the authors were

visiting the Institute for Mathematical Sciences of National University of Singapore in 2007.

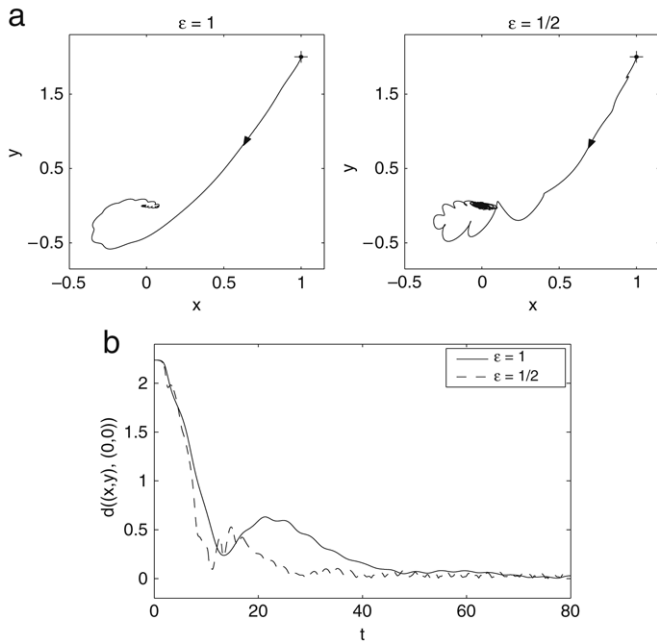


Fig. 23. Time evolution of the vortex center under an anisotropic inhomogeneous external potential (5.2) with $\gamma_x = 1$ and $\gamma_y = 5$. (a) trajectories for different ε ; and (b) distance between the vortex center and the origin.

References

- [1] J.R. Abo-Shaeer, C. Raman, J.M. Vogels, W. Ketterle, Observation of vortex lattices in Bose–Einstein condensates, *Science* 292 (2001) 476–479.
- [2] A.A. Abrikosov, On the magnetic properties of superconductors of the second group, *Sov. Phys. JETP* 5 (1957) 1174–1182.
- [3] M.H. Anderson, J.R. Ensher, M.R. Matthews, C.E. Wieman, E.A. Cornell, Observation of Bose–Einstein condensation in a dilute atomic vapor, *Science* 269 (1995) 198.
- [4] I. Aranson, L. Kramer, The world of the complex Ginzburg–Landau equation, *Rev. Modern Phys.* 74 (2002) 99–133.
- [5] W. Bao, Numerical methods for the nonlinear Schrödinger equation with nonzero far field conditions, *Methods Appl. Anal.* 11 (2004) 367–388.
- [6] W. Bao, Q. Du, Y. Zhang, Dynamics of rotating Bose–Einstein condensates and their efficient and accurate numerical computation, *SIAM J. Appl. Math.* 66 (2006) 758–786.
- [7] W. Bao, D. Jaksch, P.A. Markowich, Numerical solution of the Gross–Pitaevskii equation for Bose–Einstein condensation, *J. Comput. Phys.* 187 (2003) 318–342.
- [8] W. Bao, P.A. Markowich, H. Wang, Ground, symmetric and central vortex states in rotating Bose–Einstein condensates, *Comm. Math. Sci.* 3 (2005) 57–88.
- [9] W. Bao, Y. Zhang, Dynamics of the ground state and central vortex states in Bose–Einstein condensation, *Math. Models Methods Appl. Sci.* 15 (2005) 1863–1896.
- [10] Y. Castin, Z. Hadzibabic, S. Stock, J. Dalibard, S. Stringari, Quantized vortices in the ideal Bose gas: A physical realization of random polynomials, *Phys. Rev. Lett.* 96 (2006) article 040405.
- [11] Q. Du, M. Gunzburger, J. Peterson, Analysis and approximation of the Ginzburg–Landau model of superconductivity, *SIAM Rev.* 34 (1992) 54–81.
- [12] W. E, Dynamics of vortices in Ginzburg–Landau theories with applications to superconductivity, *Physica D* 77 (1994) 383–404.
- [13] R. Feynman, Application of Quantum Mechanics to Liquid Helium, in: *Progress in Low Temperature Physics*, vol. 1, North-Holland, Amsterdam, 1955, pp. 17–53.
- [14] J. Iaia, H. Warchall, Encapsulated-vortex solutions to equivariant wave equations existence, *SIAM J. Math. Anal.* 30 (1999) 118–139.
- [15] R.L. Jerrard, Vortex dynamics for the Ginzburg–Landau wave equation, *Calc. Var. Partial Differential Equations* 9 (1999) 1–30.
- [16] H.Y. Jian, B.H. Song, Vortex dynamics of Ginzburg–Landau equations in inhomogeneous superconductors, *J. Differential Equations* 170 (2001) 123–141.
- [17] K.T. Kapale, J.P. Dowling, Vortex phase qubit: Generating arbitrary, counterrotating, coherent superpositions in Bose–Einstein condensates via optical angular momentum beams, *Phys. Rev. Lett.* 95 (2005) article 173601.
- [18] K. Kasamatsu, M. Tsubota, Dynamical vortex phases in a Bose–Einstein condensate driven by a rotating optical lattice, *Phys. Rev. Lett.* 97 (2006) article 240404.
- [19] A. Klein, D. Jaksch, Y. Zhang, W. Bao, Dynamics of vortices in weakly interacting Bose–Einstein condensates, *Phys. Rev. A* 76 (2007) article 043602.
- [20] O. Lange, B.J. Schroers, Unstable manifolds and Schrödinger dynamics of Ginzburg–Landau vortices, *Nonlinearity* 15 (2002) 1471–1488.
- [21] A.E. Leanhardt, A. Gorlitz, A.P. Chikkatur, D. Kielpinski, Y. Shin, D.E. Pritchard, W. Ketterle, Imprinting vortices in a Bose–Einstein condensate using topological phases, *Phys. Rev. Lett.* 89 (2002) article 190403.
- [22] F.-H. Lin, Vortex dynamics for the nonlinear wave equation, *Comm. Pure Appl. Math.* 52 (1999) 737–761.
- [23] F.-H. Lin, J.X. Xin, On the dynamical law of the Ginzburg–Landau vortices on the plane, *Comm. Pure Appl. Math.* LII (1999) 1189–1212.
- [24] M.R. Matthews, B.P. Anderson, P.C. Haljan, D.S. Hall, C.E. Wieman, E.A. Cornell, Vortices in a Bose–Einstein condensate, *Phys. Rev. Lett.* 83 (1999) 2498–2501.
- [25] J.C. Neu, Vortices in complex scalar fields, *Physica D* 43 (1990) 385–406.
- [26] J.C. Neu, Vortex dynamics of the nonlinear wave equation, *Physica D* 43 (1990) 407–420.
- [27] Y.N. Ovchinnikov, I.M. Sigal, The Ginzburg–Landau equation III. vortex dynamics, *Nonlinearity* 11 (1998) 1277–1294.
- [28] Y.N. Ovchinnikov, I.M. Sigal, Asymptotic behavior of solutions of Ginzburg–Landau and related equations, *Rev. Math. Phys.* 12 (2000) 287–299.
- [29] L.P. Pitaevskii, S. Stringari, *Bose–Einstein Condensation*, Clarendon Press, 2003.
- [30] D.S. Rokhsar, Vortex stability and persistent currents in trapped Bose gases, *Phys. Rev. Lett.* 79 (1997) 2164–2167.
- [31] D.V. Skryabin, W.J. Firth, Dynamics of self-trapped beams with phase dislocation in saturable Kerr and quadratic nonlinear media, *Phys. Rev. E* 58 (1998) 3916–3930.
- [32] L.T. Vuong, T.D. Grow, A. Ishaaya, A.L. Gaeta, G.W. Hooft, E.R. Eliel, G. Fibich, Collapse of optical vortices, *Phys. Rev. Lett.* 96 (2006) article 133901.
- [33] M.I. Weinstein, J. Xin, Dynamics stability of vortex solutions of Ginzburg–Landau and nonlinear Schrödinger equations, *Comm. Math. Phys.* 180 (1996) 389–428.
- [34] Y. Zhang, W. Bao, Q. Du, Numerical simulation of vortex dynamics in Ginzburg–Landau–Schrödinger equation, *European J. Appl. Math.* 18 (2007) 607–630.
- [35] Y. Zhang, W. Bao, Q. Du, The dynamics and interaction of quantized vortices in Ginzburg–Landau–Schrödinger equation, *SIAM J. Appl. Math.* 67 (2007) 1740–1775.
- [36] Y. Zhang, W. Bao, H.L. Li, Dynamics of rotating two-component Bose–Einstein condensates and its efficient computation, *Physica D* 234 (2007) 49–69.